②

AD-A207 822

NAVAL POSTGRADUATE SCHOOL
Monterey, California

THESIS

THE EFFECT OF AUTOPILOT CONFIGURATION
ON MISSILE RESPONSE

by

Kenneth E. Cockerham

March 1989

Thesis Advisor   Harold A. Titus

DTIC
ELECTE
MAY 17 1989
S   H

89 5 17 042

REPORT DOCUMENTATION PAGE

1a Report Security Classification Unclassified			1b Restrictive Markings			
2a Security Classification Authority			3 Distribution Availability of Report			
2b Declassification Downgrading Schedule			Approved for public release: distribution is unlimited.			
4 Performing Organization Report Number(s)			5 Monitoring Organization Report Number(s)			
6a Name of Performing Organization Naval Postgraduate School		6b Office Symbol (if applicable) 32	7a Name of Monitoring Organization Naval Postgraduate School			
6c Address (city, state, and ZIP code) Monterey, CA 93943-5000			7b Address (city, state, and ZIP code) Monterey, CA 93943-5000			
8a Name of Funding Sponsoring Organization		8b Office Symbol (if applicable)	9 Procurement Instrument Identification Number			
8c Address (city, state, and ZIP code)			10 Source of Funding Numbers			
			Program Element No	Project No	Task No	Work Unit Accession No
11 Title (include security classification) THE EFFECT OF AUTOPILOT CONFIGURATION ON MISSILE RESPONSE						
12 Personal Author(s) Kenneth E. Cockerham						
13a Type of Report Master's Thesis	13b Time Covered From To		14 Date of Report (year, month, day) March 1989		15 Page Count 75	
16 Supplementary Notation The views expressed in this thesis are those of the author and do not reflect the official policy or position of the Department of Defense or the U.S. Government.						

17 Cosati Codes			18 Subject Terms (continue on reverse if necessary and identify by block number)
Field	Group	Subgroup	autopilot, missile

19 Abstract (continue on reverse if necessary and identify by block number)

A comparison of two different autopilot configurations and their effect on missile response is presented. The comparison includes the steps taken in determining missile parameters from wind tunnel data and flight condition data. The missile parameters are coupled with two different autopilot configurations to determine any significant advantage of one configuration over the other. Pole placement is used in determining required autopilot feedback and feed forward gains. Simulations of each autopilot are conducted and the responses are compared. Keywords: autopilot: missile theses; (KR)

20 Distribution Availability of Abstract ☒ unclassified unlimited ☐ same as report ☐ DTIC users	21 Abstract Security Classification Unclassified	
22a Name of Responsible Individual Harold A. Titus	22b Telephone (include Area code) (408) 646-2560	22c Office Symbol 62Ts

DD FORM 1473,84 MAR

83 APR edition may be used until exhausted
All other editions are obsolete

The Effect of Autopilot Configuration
on Missile Response

by

Kenneth E. Cockerham
Captain, United States Army
B.S., University of Tennessee at Chattanooga, 1979

Submitted in partial fulfillment of the
requirements for the degree of

MASTER OF SCIENCE IN ELECTRICAL ENGINEERING

from the

NAVAL POSTGRADUATE SCHOOL
March 1989
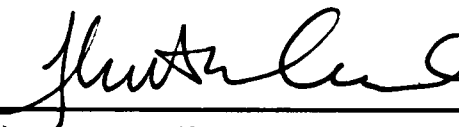
Author: _____
Kenneth E. Cockerham
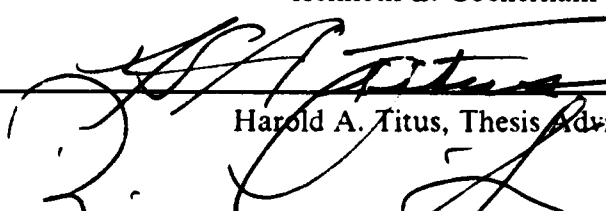
Approved by: _____
Harold A. Titus, Thesis Advisor
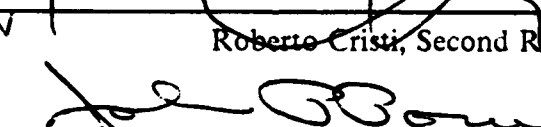
_____
Roberto Cristi, Second Reader
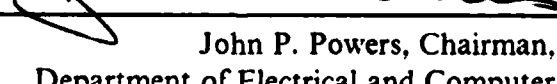
_____
John P. Powers, Chairman,
Department of Electrical and Computer Engineering
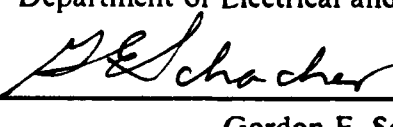
_____
Gordon E. Schacher,
Dean of Science and Engineering

ii

ABSTRACT

A comparison of two different autopilot configurations and their effect on missile response is presented. The comparison includes the steps taken in determining missile parameters from wind tunnel data and flight condition data. The missile parameters are coupled with two different autopilot configurations to determine any significant advantage of one configuration over the other. Pole placement is used in determining required autopilot feedback and feed forward gains. Simulations of each autopilot are conducted and the responses are compared.

Accession For		
NTIS GRA&I		☐
DTIC TAB		☑
Unannounced		☐
Justification		
By		
Distribution/		
Availability Codes		
Dist	Avail and/or Special	
A-1		

TABLE OF CONTENTS

LIST OF TABLES

LIST OF FIGURES

I. INTRODUCTION

The purpose of an autopilot in a missile is to cause the missile to maintain stability as it travels along its flight path. Commonly the autopilot provides stability about the missile's roll, yaw and pitch axes. Autopilots generally use displacement gyros with feedback being provided by electronic sensors which detect axial displacement due to missile rotation about one or more of the above mentioned axes.

Autopilots, as with most other man-made devices, can be constructed in a variety of different configurations. Some configurations may have advantages over others in terms of parameters such as cost, weight or effectiveness, to name a few.

In this research paper two pitch axis autopilot configurations are compared. The first is a three loop autopilot configuration, employing body rate feedback, lateral acceleration feedback and an additional synthetic stability feedback loop as depicted in Figure 1.
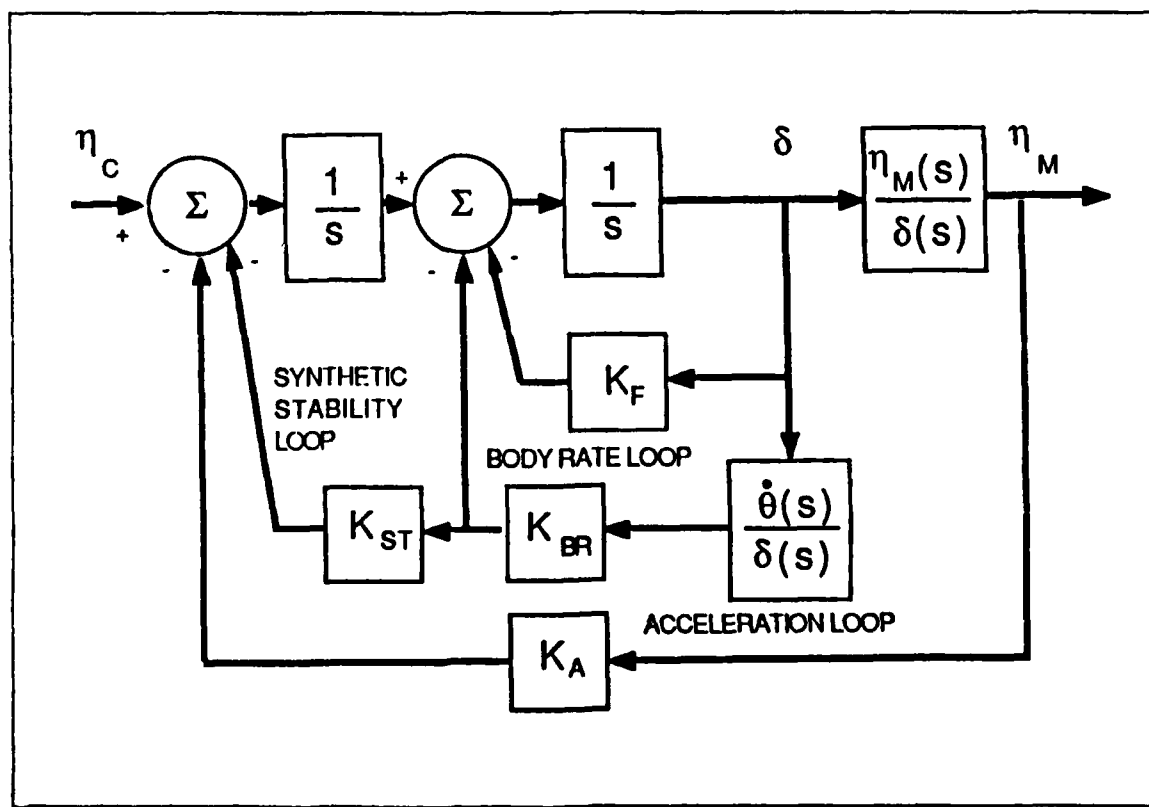
Figure 1.   Autopilot Configuration 1

The second is a two-loop autopilot configuration, employing proportional plus integral compensation in the feed forward path with body rate and lateral acceleration feedback as shown in Figure 2.
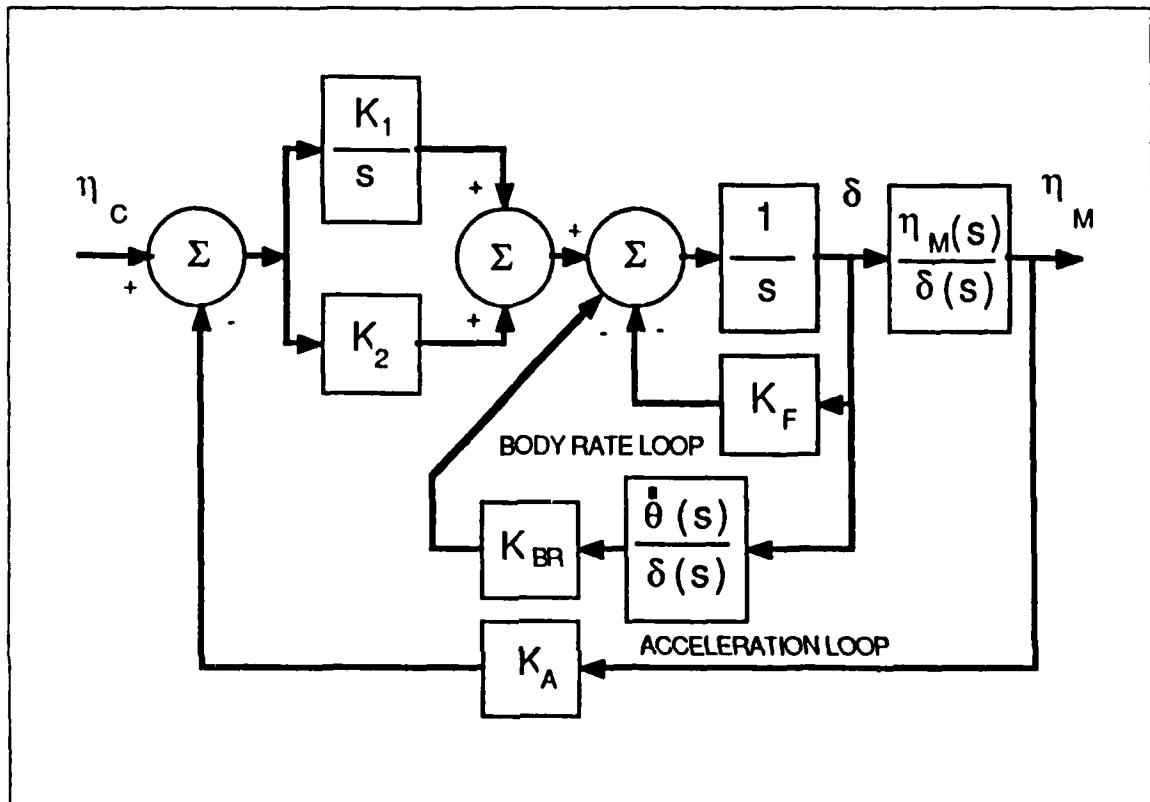
Figure 2. Autopilot Configuration 2

In these two figures η_c is the commanded lateral acceleration in the pitch plane, η_M is the measured lateral acceleration in the pitch plane, δ is the missile control surface deflection angle and θ is the missile pitch angle rate. All the subscripted K variables are gains which are constant at each design point.

The purpose of the comparison of the two autopilot configurations is to determine what advantage, if any, one may have over the other in terms of missile response. Comparisons are made of the two autopilots for three different sets of flight conditions. Each set of flight conditions is referred to as a design point. For example, design point one will refer to the first set of flight conditions. These flight conditions, or design

2

points, are specified in Chapter Two. The desired autopilot response for each configuration is given as approximately 10 radians second with a damping coefficient of 0.5.

Pertinent missile parameters are derived in Chapter Two. using given wind tunnel data and flight condition data. Any needed parameters which cannot be derived or otherwise obtained through availible information, are assumed using sound engineering judgment.

In Chapter Three the missile and autopilot transfer functions are developed. The feedback gains necessary to meet the desired autopilot design specifications are obtained allowing development of simulation studies.

Simulations are developed and conducted using Dynamic Simulation Language (DSL) in Chapter Four and the results are analyzed.

II. DEVELOPMENT OF MISSILE PARAMETERS

A. INTRODUCTION

In order to compare the effects that the two autopilot configurations have on missile performance, determination of certain missile parameters must first be made. Specifically, the transfer functions $\theta(s)/\delta(s)$ and $\eta_M(s)/\delta(s)$, which are the missile dynamics blocks in the autopilot block diagrams of Figure 1 on page 1 and Figure 2 on page 2, must be obtained.

In order to determine these transfer functions, wind tunnel data and three sets of flight condition data are provided later in this chapter. The procedures for processing this data are also presented later in this chapter.

Prior to developing the missile parameters, an explanation of the notation, terminology, and coordinate system used is in order. [Ref. 1: p. 132] Refer to Figure 3.
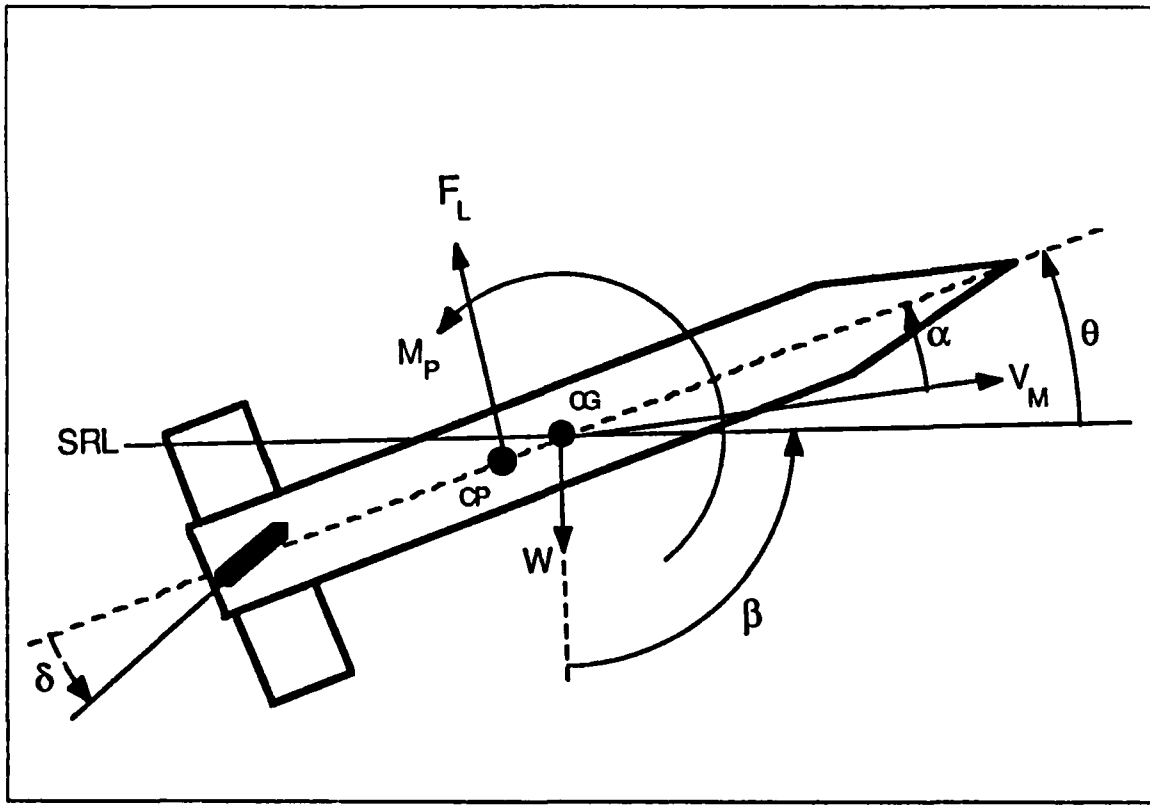
Figure 3. Missile Notation

The notation in Figure 3 represents the following:

CG is the center of gravity of the missile.

CP is the aerodynamic center of pressure of the missile.

V_M is the velocity of the missile.

SRL is the spatial reference line, a reference fixed in space.

F_L is the lift force. It is perpendicular to the velocity vector.

W is the weight of the missile.

M_P is the pitching moment. It is taken as positive in the counter-clockwise direction.

α is the angle of attack. It is the angle taken from the velocity vector to the longitudinal missile axis.

θ is the angle between the SRL and the longitudinal missile axis.

δ is the fin deflection angle. It is taken from the longitudinal missile axis to the control fin axis.

β is the angle between the gravity vector and the SRL.

Other notation and terminology will be discussed as it is introduced. It is important to remember that this problem considers only motion in the pitch plane but that similar methods may also apply to yaw motion.

B. FLIGHT CONDITION DATA

The three sets of flight condition data given in Table 1 on page 6 establish the *design points* around which the autopiloted missile will be examined. The flight condition data will be used, in conjunction with wind tunnel data presented in the next section, to establish the missile parameters and autopilot gains necessary to develop and conduct simulations of the autopiloted missile.

Some manipulation of the flight condition data is required in order for it to be used. These conversions and calculations will be made as necessary and explained when used.

Table 1. FLIGHT CONDITIONS AT THREE DESIGN POINTS

DESIGN POINT 1
T   = Time (referenced to launch) = 9.5 s Alt = Altitude = 4.993 km V   = Velocity = 1112.4 m/s M   = Mass = 450 kg q   = Dynamic Pressure = 455642 N/m² I   = Moment of Inertia = 720 kg m² Power On CP is 265 cm aft of nose
DESIGN POINT 2
T   = 18.5 s Alt = 13.54 km V   = 1086.4 m/s M   = 370 kg q   = 146829 N/m² I   = 693 kg m² Power Off CP is 265 cm aft of nose
DESIGN POINT 3
T   = 22.5 s Alt = 17.82 km V   = 934.5 m/s M   = 365 kg q   = 54637 N/m² I   = 687 kg m² Power Off CP is 266 cm aft of nose

C. WIND TUNNEL DATA

The wind tunnel data presented in this section will be instrumental in determining missile parameters. The data, shown in Table 10 on page 37 through Table 13 on page 40, are extracted from the complete wind tunnel data set for the missile used in this research paper. These data, as well as the three sets of flight condition data contained in Table 1, were provided by the U.S. Army's Missile and Space Intelligence Center (MSIC).

The first two sets of wind tunnel data are the axial force coefficients. These are given in Table 10 and Table 11 for the *Power On* and *Power Off* cases.

The third set of wind tunnel data is the normal force coefficients. These data in Table 12 on page 39 will be used, along with the axial force coefficient data to calculate the lift and drag of the missile at the design points.

The final set of wind tunnel data is the pitching moment coefficients. These data, in Table 13 on page 40 will be used to determine the pitching dynamics of the missile.

D. WIND TUNNEL DATA INTERPOLATION

To enter the wind tunnel data at the desired design point, the Mach number must be calculated from the flight condition data. Using given missile velocity and altitude, with temperature obtained from gas tables and graphs found in [Refs. 2,3], the Mach number for each design point is calculated by gas law equation techniques. These calculations are not included here. The Mach number at each design point is given in Table 2.

Table 2. MACH NUMBERS AT DESIGN POINTS

DESIGN POINT	MACH NUMBER
1	3.48
2	3.68
3	3.17

The availability of the Mach number at each design point allows entry of the wind tunnel data and interpolation of the various coefficients for each design point. The interpolation of the wind tunnel data at each design point is accomplished using a simple linear interpolation scheme. The interpolation provides the coefficients at each design point. These interpolated coefficients are given in Table 14 on page 41 through Table 17 on page 43.

E. CALCULATION OF LIFT AND DRAG COEFFICIENTS

Once the axial and normal force coefficients at the design points have been determined the lift and drag coefficients can be calculated. The lift force, F_L, and drag force, F_D, are related to the normal force, F_N, and the axial force, F_A, by the trigonometric

7

relationships

$$F_L = F_N \cos\alpha - F_A \sin\alpha \qquad (2.1)$$

and

$$F_D = F_N \sin\alpha + F_A \cos\alpha. \qquad (2.2)$$

These relationships are depicted in Figure 4 below.
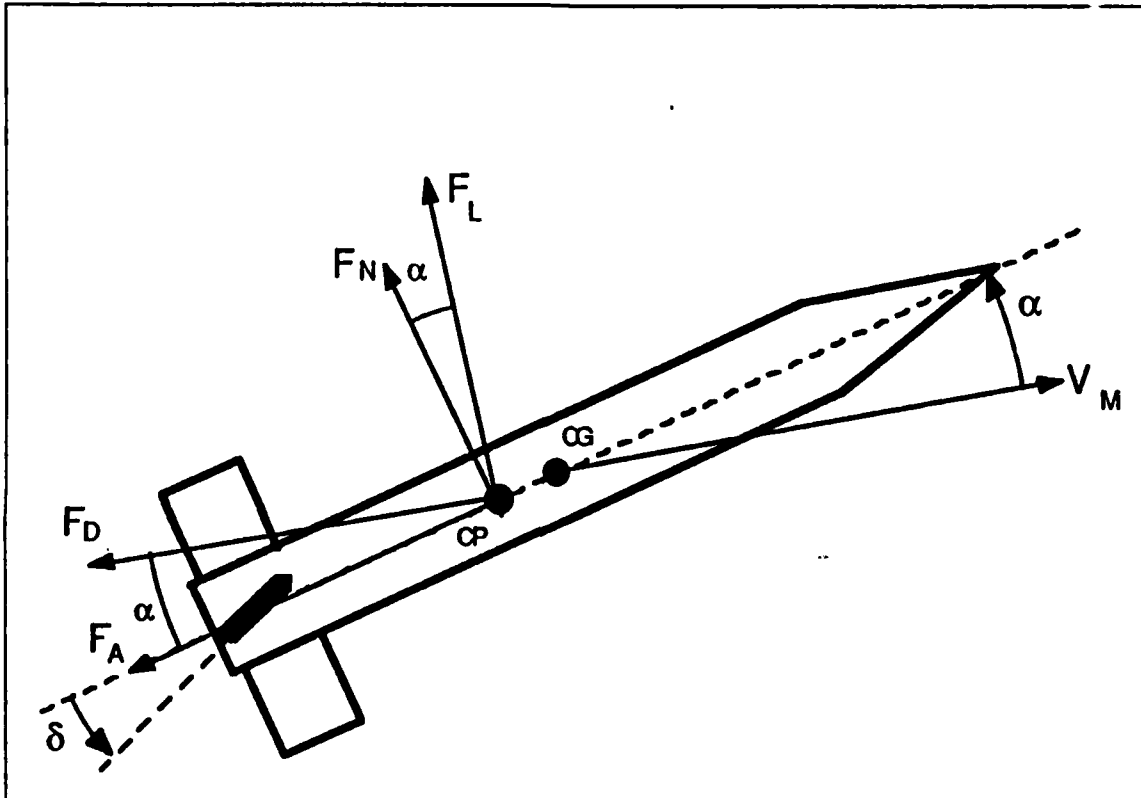
Figure 4.   Force Relationships

Since the coefficients are dimensionless representations of the forces, the same relationships apply. Specifically,

$$C_L = C_N \cos\alpha - C_A \sin\alpha \qquad (2.3)$$

and

$$C_D = C_N \sin\alpha + C_A \cos\alpha \qquad (2.4)$$

8

where C_L is the lift coefficient, C_D is the drag coefficient, C_A is the axial force coefficient, and C_N is the normal force coefficient. [Ref. 1: p. 134]

The application of these equations to the interpolated wind tunnel data in Appendix B renders lift and drag coefficients at the design points. These lift and drag coefficients are tabulated in Appendix C.

F. ANALYSIS OF WIND TUNNEL DATA

There are four missile parameters which are of interest in the development of the missile dynamics transfer functions. These parameters are: $F_{L\alpha}$, which is the lift force per angle of attack, $F_{L\delta}$, which is the lift force per fin deflection angle, $M_{P\alpha}$, which is the moment about the center of gravity per angle of attack, and $M_{P\delta}$, which is the moment about the center of gravity per fin deflection angle.

These parameters can be determined from their corresponding coefficients and a few physical dimensions of the missile. The corresponding coefficients are discussed in the paragraphs which follow.

$C_{L\alpha}$ is the lift coefficient per angle of attack. It is determined by graphing the lift coefficients against the angle of attack and approximating the slope of the nearly linear graph.

$C_{L\delta}$ is the lift coefficient per fin deflection angle. It is determined by graphing the lift coefficients against the fin deflection angle and approximating the slope.

Similarly, $C_{M\alpha}$ and $C_{M\delta}$ are the pitching moment coefficients per angle of attack and fin deflection angle, respectively. They too are obtained by graphing the coefficients against the angles and approximating the slope of the resulting graph.

The graphs of all the coefficients versus corresponding angles are contained in Appendix D. The graphs are made for each set of coefficients at each of the three design points. The coefficients $C_{L\alpha}$, $C_{L\delta}$, $C_{M\alpha}$, and $C_{M\delta}$ are tabulated in Table 3 on page 10.

9

Table 3. COEFFICIENTS DUE TO ANGLE OF ATTACK AND FIN DEFLECTION ANGLE

	DESIGN POINT 1	DESIGN POINT 2	DESIGN POINT 3
C_{Lx}	0.27	0.25	0.28
$C_{L\delta}$	0.03	0.02	0.03
C_{Mx}	-0.15	-0.12	-0.20
$C_{M\delta}$	-0.17	-0.15	-0.22

G. CALCULATION OF MISSILE PARAMETERS

As mentioned in the preceding section, the parameters of interest are F_{Lx}, $F_{L\delta}$, M_{Px}, and $M_{P\delta}$. With knowledge of the lift and moment coefficients previously obtained, and knowledge of some basic physical dimensions of the missile, these parameters are determined. The necessary missile dimensions are shown in Figure 5. These missile dimensions were provided by the Missile and Space Intelligence Center.

SIDE VIEW

5.3 m

DIAMETER 0.38 m

END VIEW
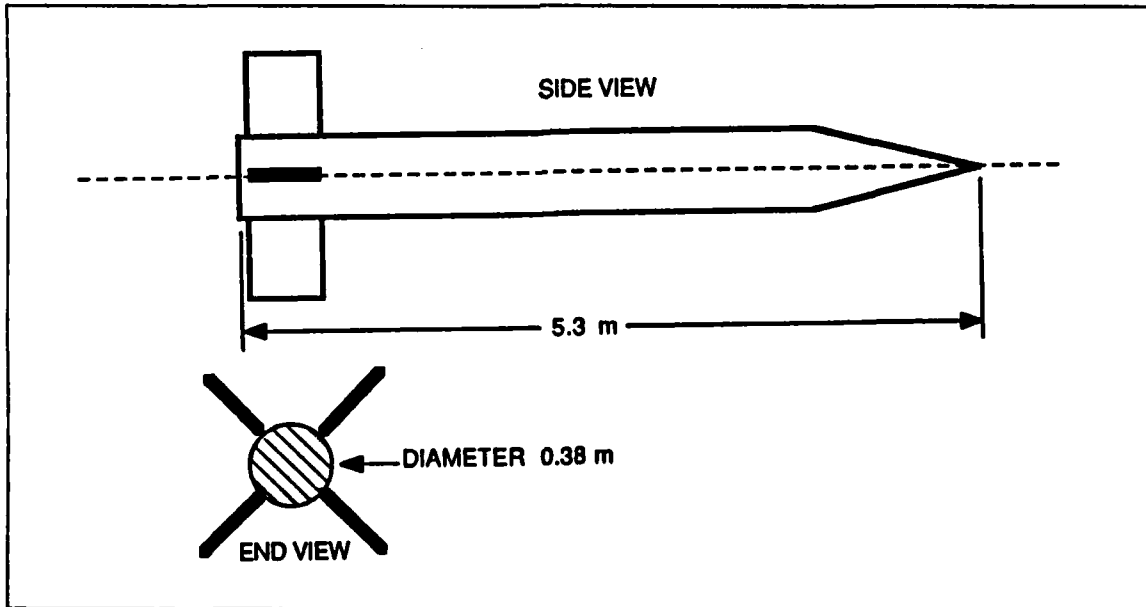
Figure 5. Missile Dimensions

The equations used to determine the missile parameters from the coefficients are:

$$\Gamma_{L\alpha} = C_{L\alpha} q A, \qquad (2.5)$$

$$\Gamma_{L\delta} = C_{L\delta} q A, \qquad (2.6)$$

$$M_{P\alpha} = C_{M\alpha} q A c, \qquad (2.7)$$

and

$$M_{P\delta} = C_{M\delta} q A c \qquad (2.8)$$

where q is the dynamic pressure, provided in the flight conditions, A is the missile characteristic area, and c is the characteristic length. The characteristic area, A, is taken as

$$A = \pi \frac{d^2}{4} \qquad (2.9)$$

where d is the missile diameter, 38 cm, as given in Figure 19 above. The characteristic length is taken as the missile diameter. [Ref. 1: p. 134]

Applying the above equations to the known coefficients produces the missile parameters at the three design points. Use of these parameters in later chapters requires that they be given in force or moment per radian rather than per degree. This conversion is made mulitplying each parameter by $180/\pi$. These converted parameters are tabulated in Table 4 on page 12.

Knowledge of these missile parameters will enable the derivation of the missile dynamics transfer functions in the following chapter.

Table 4. MISSILE PARAMETERS AT DESIGN POINTS

PARAMETER	DESIGN POINT 1	DESIGN POINT 2	DESIGN POINT 3
F_{Lx}	799276 N	238350 N	99695 N
$F_{L\delta}$	88808 N	19080 N	10657 N
M_{Px}	-168736 Nm	-43545 Nm	-26986 Nm
$M_{P\delta}$	-191368 Nm	-54431 Nm	-29679 Nm

12

III. DETERMINATION OF TRANSFER FUNCTIONS

A. OVERVIEW

In this chapter, the missile parameters obtained in the previous chapter are applied to the equations of motion which govern the flight of the missile. From this, the missile dynamics transfer functions, $\theta(s)/\delta(s)$ and $\eta_M(s)/\delta(s)$, are derived. By then inserting these two missile dynamics transfer functions into the two autopilot transfer functions, the complete autopilot transfer functions can be expressed in terms of missile parameters and feedback gains.

B. MISSILE DYNAMICS TRANSFER FUNCTIONS

Consider the forces and moments acting on a missile while in flight. These are depicted in Figure 3 on page 4. Summing the forces in the transverse direction, that is perpendicular to the velocity vector, yields

$$\sum F_T = \eta_M m = F_L - W \sin(\beta + \theta - \alpha). \tag{3.1}$$

Since

$$F_L = F_{L\alpha}\alpha + F_{L\delta}(\delta + \alpha), \tag{3.2}$$

the substitution is made yielding

$$\eta_M m = F_{L\alpha}\alpha + F_{L\delta}(\delta + \alpha) - W \sin(\beta + \theta - \alpha). \tag{3.3}$$

Dividing through by the mass, m, yields the lateral acceleration, η_M .

$$\eta_M = \frac{F_{L\alpha}}{m}\alpha + \frac{F_{L\delta}}{m}(\delta + \alpha) - \frac{W}{m}\sin(\beta + \theta - \alpha) \tag{3.4}$$

The weight of the missile is neglected at this point for simplicity. The missile's weight would affect the lateral acceleration of the missile most when the angle $(\beta + \theta - \alpha)$ is 90 or 270 degrees. At this angle the contribution to lateral acceleration would be plus or minus 1 G. This effect would be offset by fin deflection and angle of

13

attack trim angles of much less than one degree at any of the three design points. Neglecting missile weight leaves the approximation

$$\eta_M \simeq \frac{F_{L\alpha}}{m}\alpha + \frac{F_{L\delta}}{m}(\delta + \alpha) = \alpha\frac{(F_{L\alpha} + F_{L\delta})}{m} + \delta\frac{(F_{L\delta})}{m} \tag{3.5}$$

which is used to determine η_M at each design point in terms of α and δ.

In a similar manner, summing moments about the center of gravity of the missile with the counter-clockwise direction being referenced as the positive direction yields

$$\sum M_{CG} = I\ddot{\theta} = M_P \tag{3.6}$$

where I is the missile's moment of inertia, θ is the missile's angular acceleration in the pitch plane, and M_P is the pitching moment. The pitching moment, M_P, is given by the equation

$$M_P = \dot{\alpha}M_{P\dot{\alpha}} + \dot{\theta}M_{P\dot{\theta}} + \alpha M_{P\alpha} + (\alpha + \delta)M_{P\delta}. \tag{3.7}$$

Since $\dot{\alpha} \simeq \dot{\theta}$ and $\ddot{\alpha} \simeq \ddot{\theta}$ the substitution is made leaving

$$M_P = \dot{\alpha}(M_{P\dot{\alpha}} + M_{P\dot{\theta}}) + \alpha(M_{P\alpha} + M_{P\delta}) + \delta(M_{P\delta}). \tag{3.8}$$

Combining and rearranging the above equations yields

$$\ddot{\alpha} - \frac{(M_{P\dot{\alpha}} + M_{P\dot{\theta}})}{I}\dot{\alpha} - \frac{(M_{P\alpha} + M_{P\delta})}{I}\alpha = \frac{M_{P\delta}}{I}\delta. \tag{3.9}$$

In Equation (3.9), the term

$$\frac{(M_{P\dot{\alpha}} + M_{P\dot{\theta}})}{I}$$

is the aerodynamic damping term. It is beyond the scope of this research paper to properly obtain this term. It is, therefore, assumed that the missile is designed with a damping coefficient of $\zeta = 0.5$. The aerodynamic damping term will be different numerically at each of the three design points and will be referred to hereafter as D. It will

be calculated later in this chapter. [Ref. 4]

Substituting D into Equation (3.9) yields

$$\ddot{\alpha} - D\dot{\alpha} - \frac{(M_{P\alpha} + M_{P\delta})}{I}\alpha = \frac{M_{P\delta}}{I}\delta. \tag{3.10}$$

Using LaPlace transforms and assuming zero initial conditions this equation transforms into

$$s^2\alpha(s) - Ds\alpha(s) - \frac{(M_{P\alpha} + M_{P\delta})}{I}\alpha(s) = \frac{M_{P\delta}}{I}\delta(s). \tag{3.11}$$

Rearranging, this becomes

$$\frac{\alpha(s)}{\delta(s)} = \frac{\dfrac{M_{P\delta}}{I}}{s^2 - Ds - \dfrac{(M_{P\alpha} + M_{P\delta})}{I}}. \tag{3.12}$$

Multiplying both sides by s renders

$$\frac{s\alpha(s)}{\delta(s)} = \frac{s\dfrac{M_{P\delta}}{I}}{s^2 - Ds - \dfrac{(M_{P\alpha} + M_{P\delta})}{I}} = \frac{\dot{\alpha}(s)}{\delta(s)}. \tag{3.13}$$

Since $\dot{\alpha} = \theta$,

$$\frac{\dot{\alpha}(s)}{\delta(s)} = \frac{\dot{\theta}(s)}{\delta(s)} = \frac{s\dfrac{M_{P\delta}}{I}}{s^2 - Ds - \dfrac{(M_{P\alpha} + M_{P\delta})}{I}}. \tag{3.14}$$

This transfer function is depicted in the signal flow graph of Figure 6 on page 16.
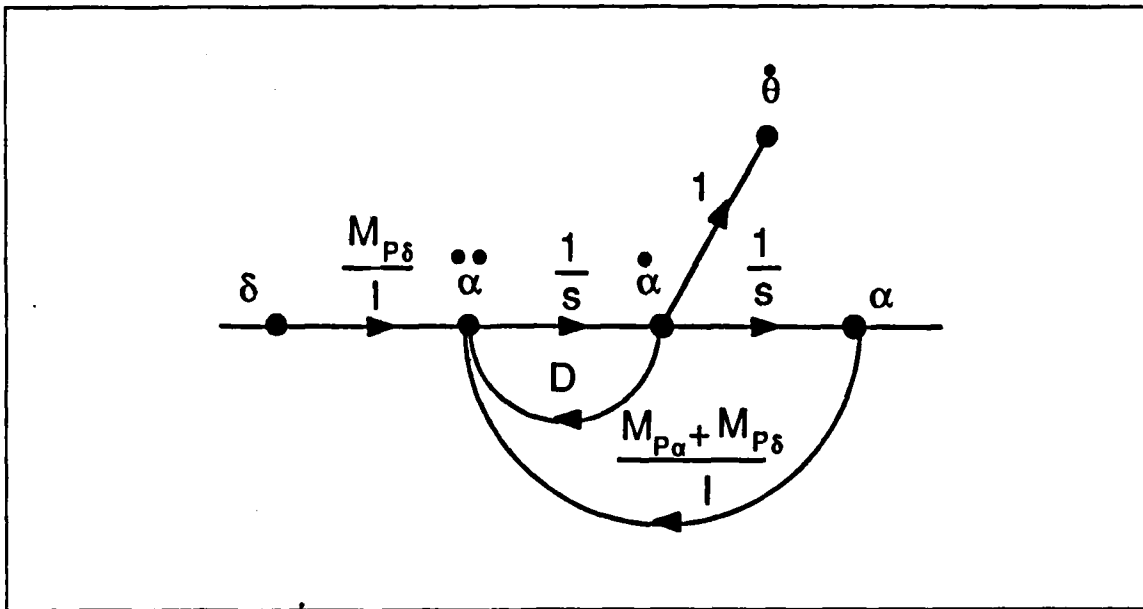
Figure 6. Pitch Transfer Function Signal Flow Graph

The aerodynamic damping term, D, is calculated for each of the three design points. The denominator of the $\theta(s)/\delta(s)$ transfer function is the characteristic equation of that system. It is in the quadratic form of $s^2 + s2\zeta\omega_n + \omega_n^2$. Equating coefficients yields

$$-D = 2\zeta\omega_n \tag{3.15}$$

and

$$\omega_n = \sqrt{-\frac{(M_{p\alpha} + M_{p\delta})}{I}}. \tag{3.16}$$

Using the missile parameters obtained in the previous chapter and the assumed value of 0.5 for ζ, the damping term, D, is calculated. The values for D are given in Table 5 on page 17. [Ref. 5: pp. 106-107]

Table 5. AERODYNAMIC DAMPING COEFFICIENTS

DESIGN POINT	DAMPING COEFFICIENT
1	-22.4
2	-11.9
3	-9.1

The other missile dynamics transfer function needed is the lateral acceleration transfer function, $\eta_M(s)/\delta(s)$. Combining the signal flow graph of Figure 6 with Equation (3.5) results in the signal flow graph of Figure 7.
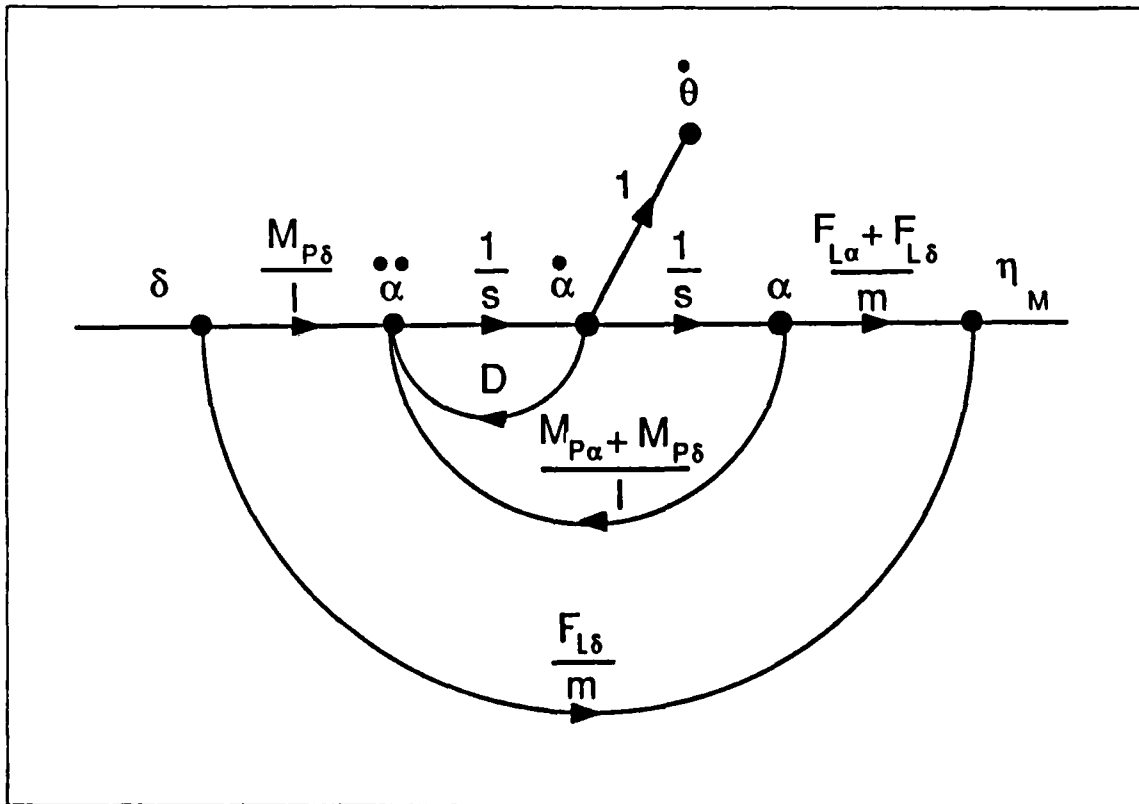
Figure 7.   Acceleration Transfer Function Signal Flow Graph

The transfer function associated with this signal flow graph is given as

$$\frac{\eta_M(s)}{\delta(s)} = \frac{\dfrac{M_{P\delta}}{I}\dfrac{(F_{L\alpha} + F_{L\delta})}{m}}{s^2 - sD - \dfrac{(M_{P\alpha} + M_{P\delta})}{I}} + \frac{F_{L\delta}}{m} \ . \tag{3.17}$$

17

The transfer functions for the missile dynamics are thus obtained. They will be used in the following section to determine the autopilot transfer functions.

C. AUTOPILOT TRANSFER FUNCTIONS

By inserting the two missile dynamics transfer functions into each of the two autopilot configuration block diagrams presented in Chapter One, and performing a few basic block diagram manipulations, the closed loop autopilot transfer functions are obtained. In both cases, the desired autopilot transfer function is $\eta_M(s)/\eta_C(s)$. For Autopilot Configuration One the transfer function is

$$\frac{\eta_M(s)}{\eta_C(s)} = \frac{\dfrac{\eta_M(s)}{\delta(s)}}{s^2 + s(K_F + K_{BR}\dfrac{\dot{\theta}(s)}{\delta(s)}) + K_{ST}K_{BR}\dfrac{\dot{\theta}(s)}{\delta(s)} + K_A} \ . \tag{3.18}$$

Expanding the missile dynamics transfer functions in the autopilot transfer function and performing extensive algebraic manipulations yields

$$G_1(s) = \frac{\eta_M(s)}{\eta_C(s)} = \frac{n_{01}s^2 + n_{11}s + n_{21}}{s^4 + d_{01}s^3 + d_{11}s^2 + d_{21}s + d_{31}} \tag{3.19}$$

where

$$n_{01} = \frac{F_{L\delta}}{m} \ ,$$

$$n_{11} = -D\frac{F_{L\delta}}{m} \ ,$$

$$n_{21} = \frac{M_{P\delta}}{I}\frac{(F_{L\alpha}+F_{L\delta})}{m} - \frac{F_{L\delta}}{m}\frac{(M_{P\alpha}+M_{P\delta})}{I} \ .$$

$$d_{01} = K_F - D \ ,$$

$$d_{11} = K_{BR}\frac{M_{P\delta}}{I} + K_A\frac{F_{L\delta}}{m} - K_F D - \frac{(M_{P\alpha}+M_{P\delta})}{I} \ ,$$

$$d_{21} = K_{ST}K_{BR}\frac{M_{P\delta}}{I} - K_F\frac{(M_{P\alpha}+M_{P\delta})}{I} - K_A D\frac{F_{L\delta}}{m} \ ,$$

and

$$d_{31} = K_A \left(\frac{M_{P\delta}}{I} \frac{(F_{L\alpha} + F_{L\delta})}{m} - \frac{F_{L\delta}}{m} \frac{(M_{P\alpha} + M_{P\delta})}{I} \right) .$$

The transfer function for Autopilot Configuration Two is obtained in a similar manner. For the second configuration

$$\frac{\eta_M(s)}{\eta_C(s)} = \frac{(K_2 s + K_1) \dfrac{\eta_M(s)}{\delta(s)}}{s^2 + s\left(K_F + K_{BR} \dfrac{\dot{\theta}(s)}{\delta(s)}\right) + K_A(K_2 s + K_1) \dfrac{\eta_M(s)}{\delta(s)}} . \tag{3.20}$$

This expands into

$$G_2(s) = \frac{\eta_M(s)}{\eta_C(s)} = \frac{n_{02} s^3 + n_{12} s^2 + n_{22} s + n_{32}}{s^4 + d_{02} s^3 + d_{12} s^2 + d_{22} s + d_{32}} \tag{3.21}$$

where

$$n_{02} = K_2 \frac{F_{L\delta}}{m} ,$$

$$n_{12} = K_1 \frac{F_{L\delta}}{m} - K_2 D \frac{F_{L\delta}}{m} ,$$

$$n_{22} = K_2 \left(\frac{M_{P\delta}}{I} \frac{(F_{L\alpha} + F_{L\delta})}{m} - \frac{F_{L\delta}}{m} \frac{(M_{P\alpha} + M_{P\delta})}{I} \right) - K_1 D \frac{F_{L\delta}}{m} ,$$

$$n_{32} = K_1 \left(\frac{M_{P\delta}}{I} \frac{F_{L\alpha} + F_{L\delta}}{m} - \frac{F_{L\delta}}{m} \frac{(M_{P\alpha} + M_{P\delta})}{I} \right) ,$$

$$d_{02} = K_F - D + K_A K_2 \frac{F_{L\delta}}{m} ,$$

$$d_{12} = K_{BR} \frac{M_{P\delta}}{I} - \frac{M_{P\alpha} + M_{P\delta}}{I} - K_F D - K_A K_2 D \frac{F_{L\delta}}{m} + K_A K_1 \frac{F_{L\delta}}{m} ,$$

$$d_{22} = K_A K_2 \left(\frac{M_{P\delta}}{I} \frac{(F_{L\alpha} + F_{L\delta})}{m} - \frac{F_{L\delta}}{m} \frac{(M_{P\alpha} + M_{P\delta})}{I} \right) - K_A K_1 D \frac{F_{L\delta}}{m} - K_F \frac{(M_{P\alpha} + M_{P\delta})}{I} ,$$

and

$$d_{32} = K_A K_1 \left(\frac{M_{P\delta}}{I} \frac{(F_{L\alpha} + F_{L\delta})}{m} - \frac{F_{L\delta}}{m} \frac{(M_{P\alpha} + M_{P\delta})}{I} \right).$$

These closed loop autopilot transfer functions will be used in the next section for system pole placement and solution of the feedback and feed forward gains.

D. POLE PLACEMENT AND GAIN DETERMINATION

As stated in Chapter One of this research paper, the desired autopilot response for both configurations is $\omega_n = 10$ with a damping coefficient $\zeta = 0.5$. These design specifications dictate a complex pair of poles in the characteristic equation whose real part is -5.0. Since the autopilots' characteristic equations are fourth order, two more poles are required to put them in the form

$$CE = (s^2 + s2\zeta\omega_n + \omega_n^2)(s + p_1)(s + p_2).$$ (3.22)

In order for the complex pair placed by design specifications to be dominant, the other two poles must lie to the left of them in the s-plane. The two additional poles are selected for simplicity as real and equal and placed at -20.0. The characteristic equation for both autopilot configurations is

$$CE = (s + 20)(s + 20)(s^2 + 10s + 100)$$

$$= s^4 + 50s^3 + 900s^2 + 8000s + 40000.$$ (3.23)

The denominators of the closed loop transfer functions, which are given by Equations (3.19) and (3.21), are the autopilot characteristic equations. The transfer function gains are solved for by first equating the coefficients of characteristic equation of above to those of Equations (3.19) and (3.21), then solving simultaneous equations for the gains. The calculated gains for Autopilot Configuration One and Autopilot Configuration Two are tabulated in Table 6 and Table 7, respectively. The determination of the autopilot gains makes it possible to simulate the response of the missile. These simulations will be conducted in the next chapter. [Refs. 6,7]

Table 6. AUTOPILOT GAINS FOR CONFIGURATION ONE

GAIN	DESIGN POINT 1	DESIGN POINT 2	DESIGN POINT 3
K_A	-0.094	-0.845	-3.06
K_F	27.6	38.1	40.9
K_{ST}	26.96	8.98	10.18
K_{BR}	0.752	-4.44	-12.37

Table 7. AUTOPILOT GAINS FOR CONFIGURATION TWO

GAIN	DESIGN POINT 1	DESIGN POINT 2	DESIGN POINT 3
$K_A K_1$	-0.094	-0.845	-3.06
$K_A K_2$	0.004	-0.057	-0.352
K_F	20.1	41.05	51.17
K_{BR}	-0.513	-7.62	-12.83

It is interesting to note that the values of K_1 and K_2 for Configuration Two, depend on the selected value of K_A. For purposes of simulation in the next chapter, K_A is chosen as unity. This results in $K_A K_1$ being equal to K_1 and $K_A K_2$ being equal to K_2 for the simulation.

IV. AUTOPILOT SIMULATION AND ANALYSIS

A. AUTOPILOT SIMULATION

In order to compare the responses of the two autopilot configurations, a simulation program was developed using IBM's Dynamic Simulation Language. [Ref. 8]

. The program simulates the step response of the autopilot transfer functions for both configurations, at all three design points. The simulation was developed from Equations (3.19) and (3.21), which describe the two autopilot transfer functions, and uses the feedback and feed forward gains tabulated in Table 6 and Table 7 on page 21. The program also incorporates a saturating limiter which limits the deflection of the control fins to ± 20°. A copy of the program listing is at Appendix E.

The program was run on the IBM 3360 mainframe computer system at the Naval Postgraduate School utilizing a Tektronix 618 Monitor and Tektronix 4631 Hard Copy Unit for graphic output.

This chapter contains the graphical results of these simulations. Figure 8 on page 23 through Figure 10 on page 25 depict the step response of Autopilot Configuration One at each of the three design points. Figure 11 on page 26 shows the parametric display of the step response of Autopilot Configuration One at all three design points. Figure 12 on page 27 through Figure 14 on page 29 depict the step response of Autopilot Configuration Two at each of the three design points. Figure 15 on page 30 displays parametrically the step response of Autopilot Configuration Two at all three design points. The parametric comparisons of the two autopilot configurations at each design point are shown in Figure 16 on page 31 through Figure 18 on page 33. The next section contains discussion and analysis of the graphical output.
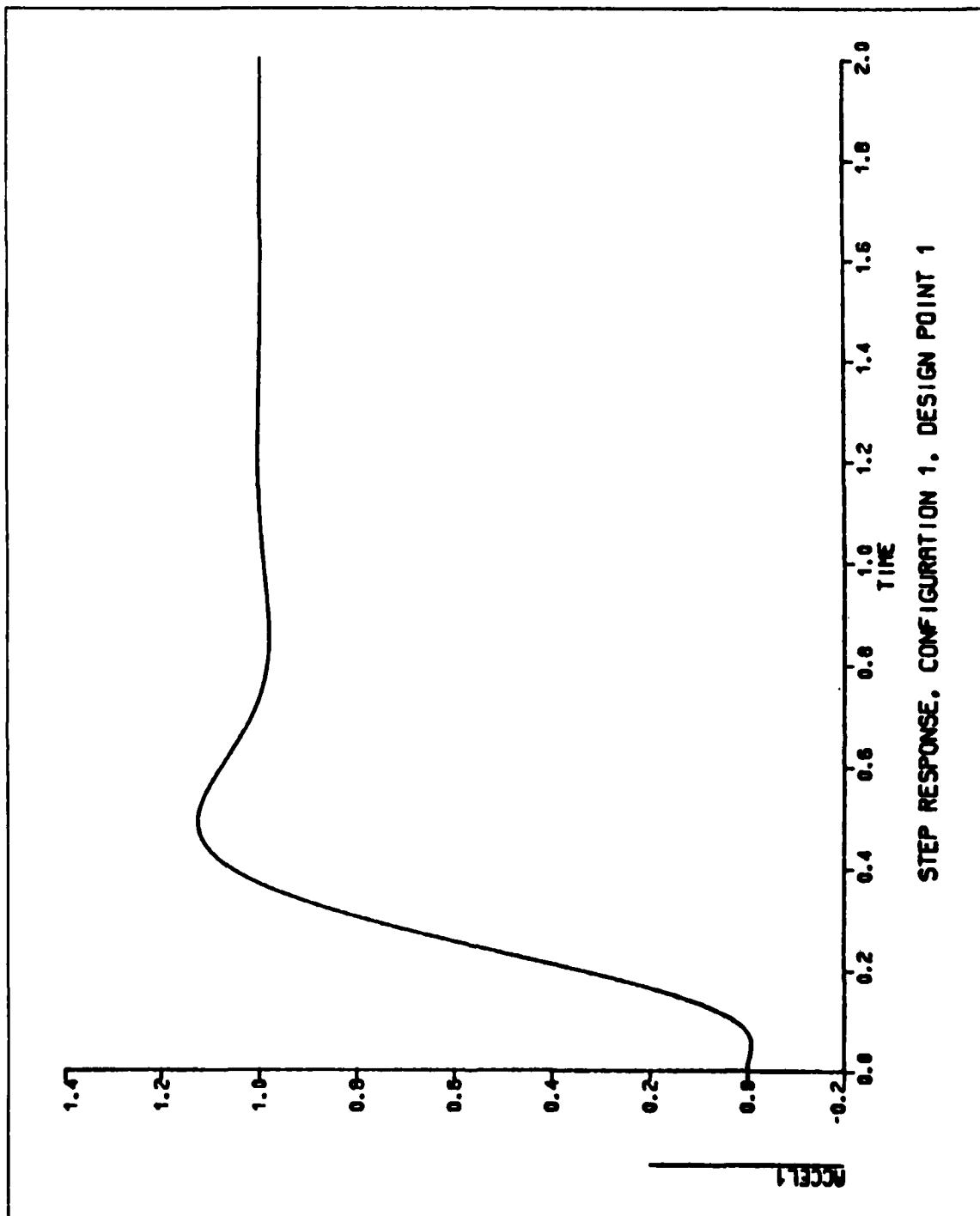
Figure 8. Step Response of Autopilot Configuration One at Design Point One
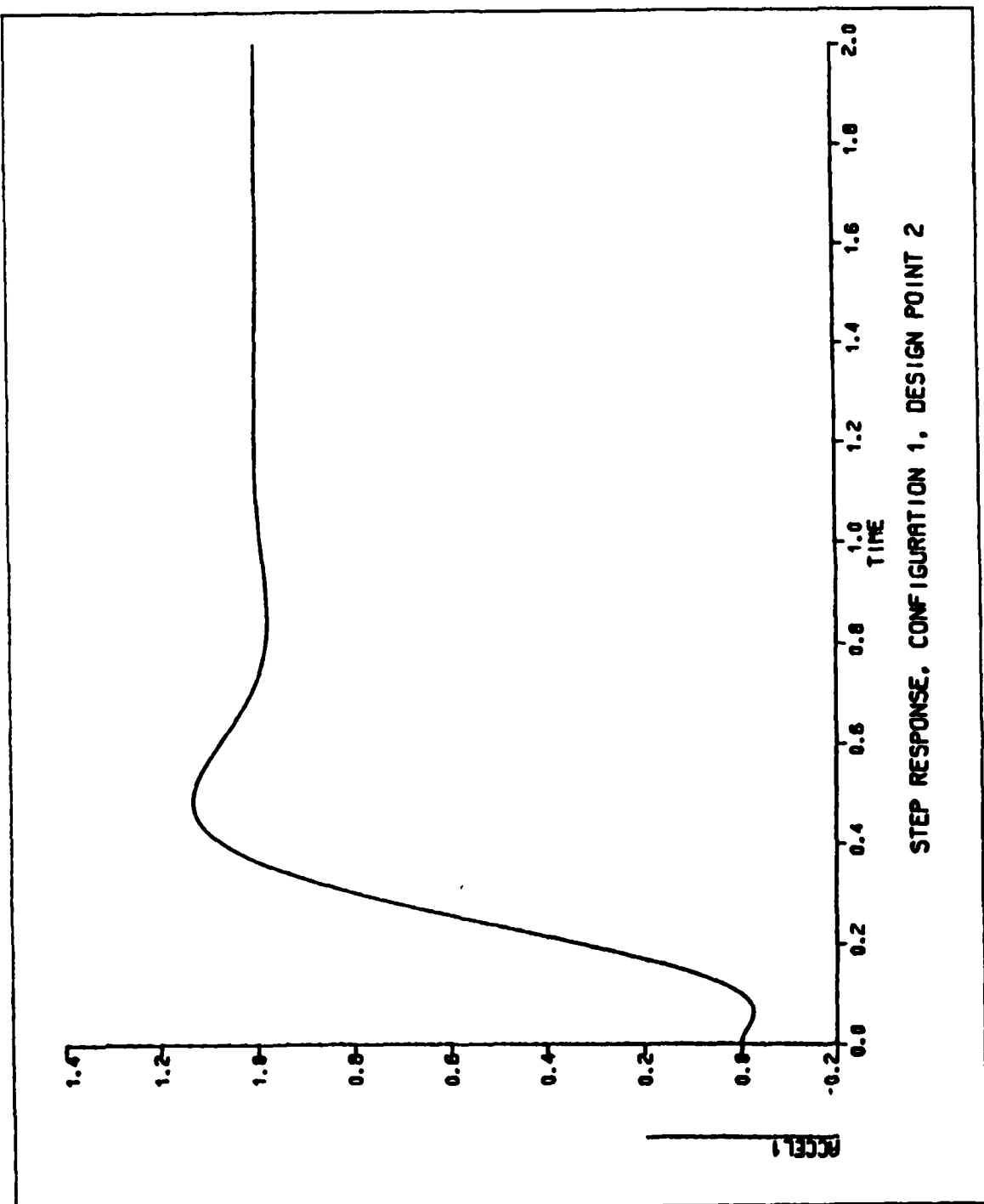
Figure 9.   Step Response of Autopilot Configuration One at Design Point Two
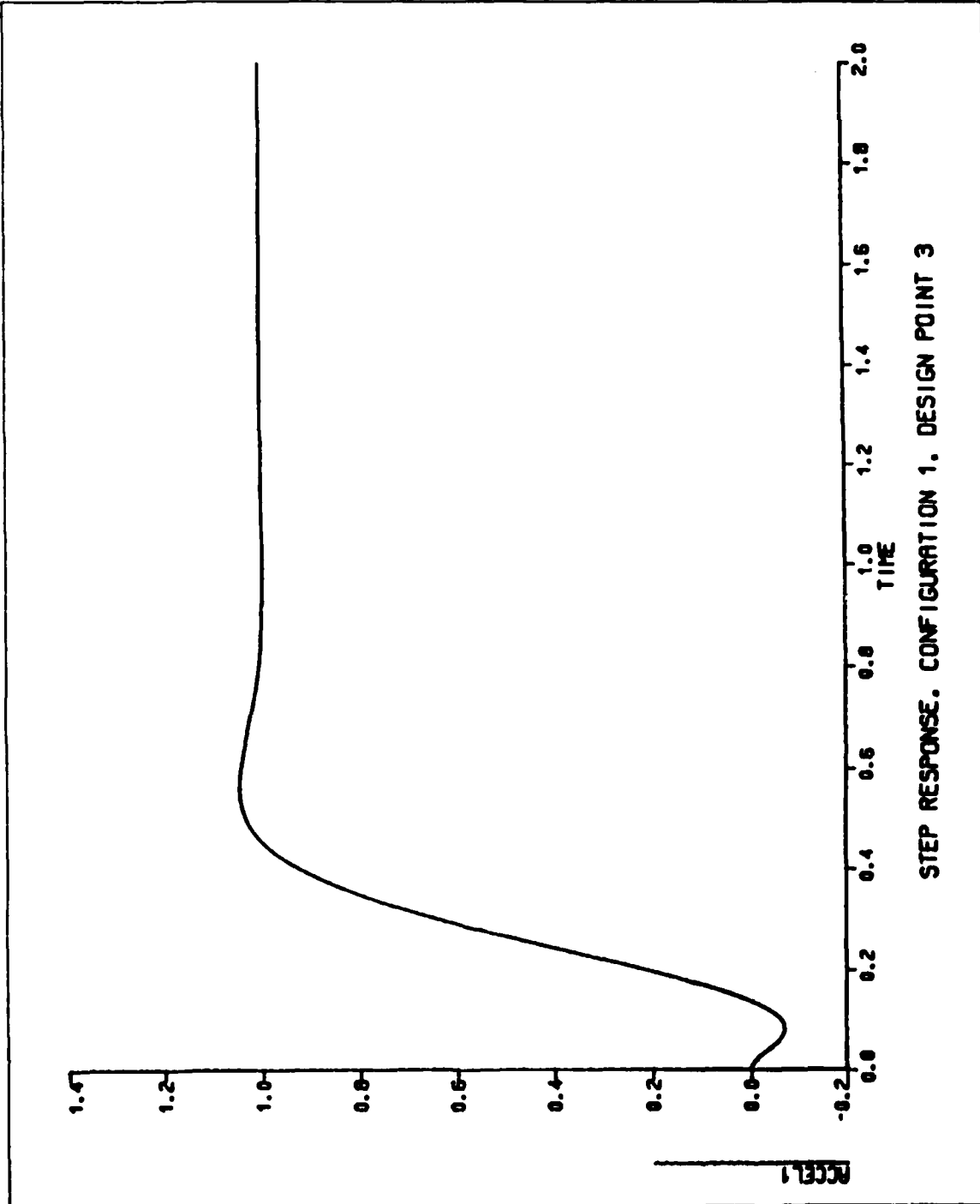
Figure 10.   Step Response of Autopilot Configuration One at Design Point Three

25
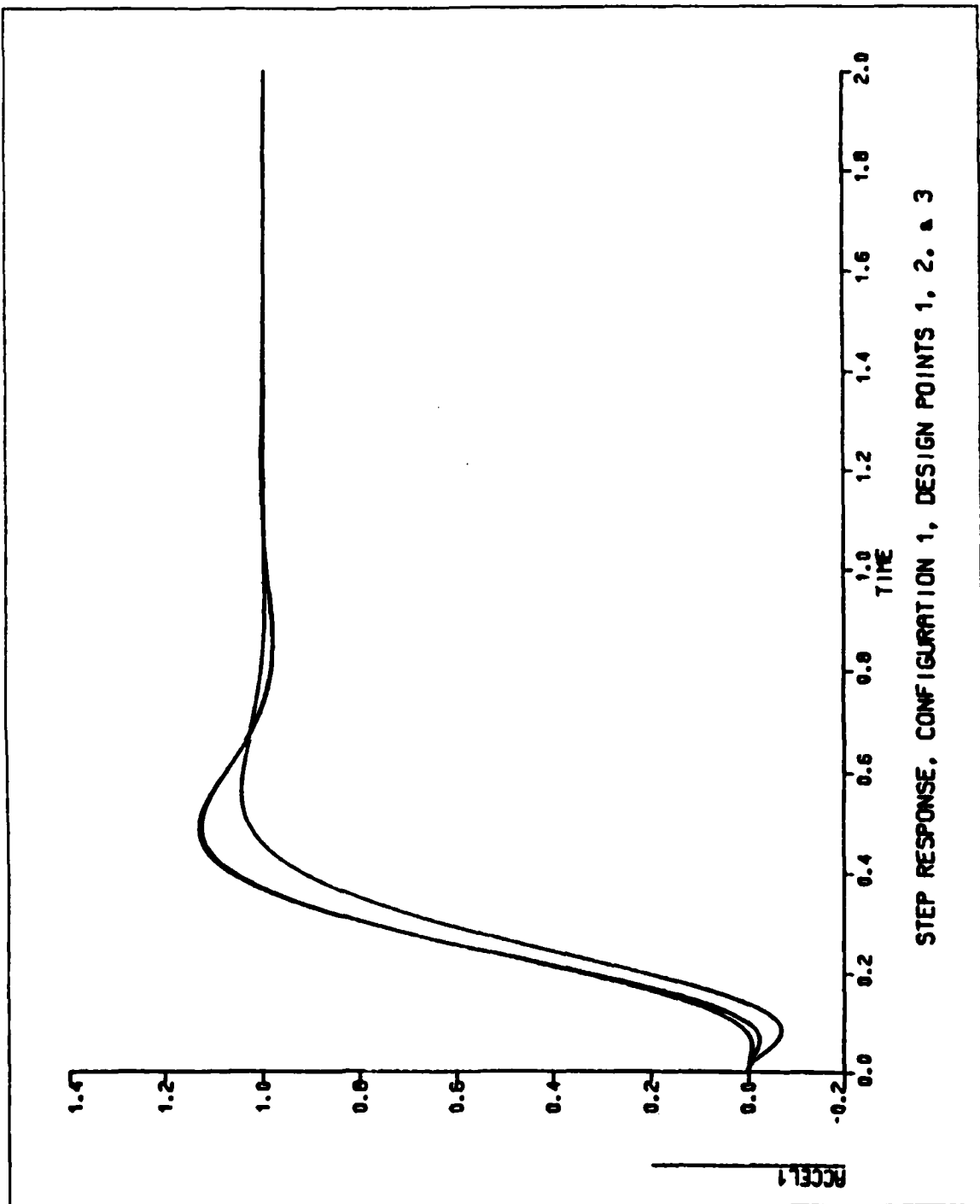
Figure 11.   Parametric Comparison of the Step Response of Autopilot Configuration
One at Three Design Points
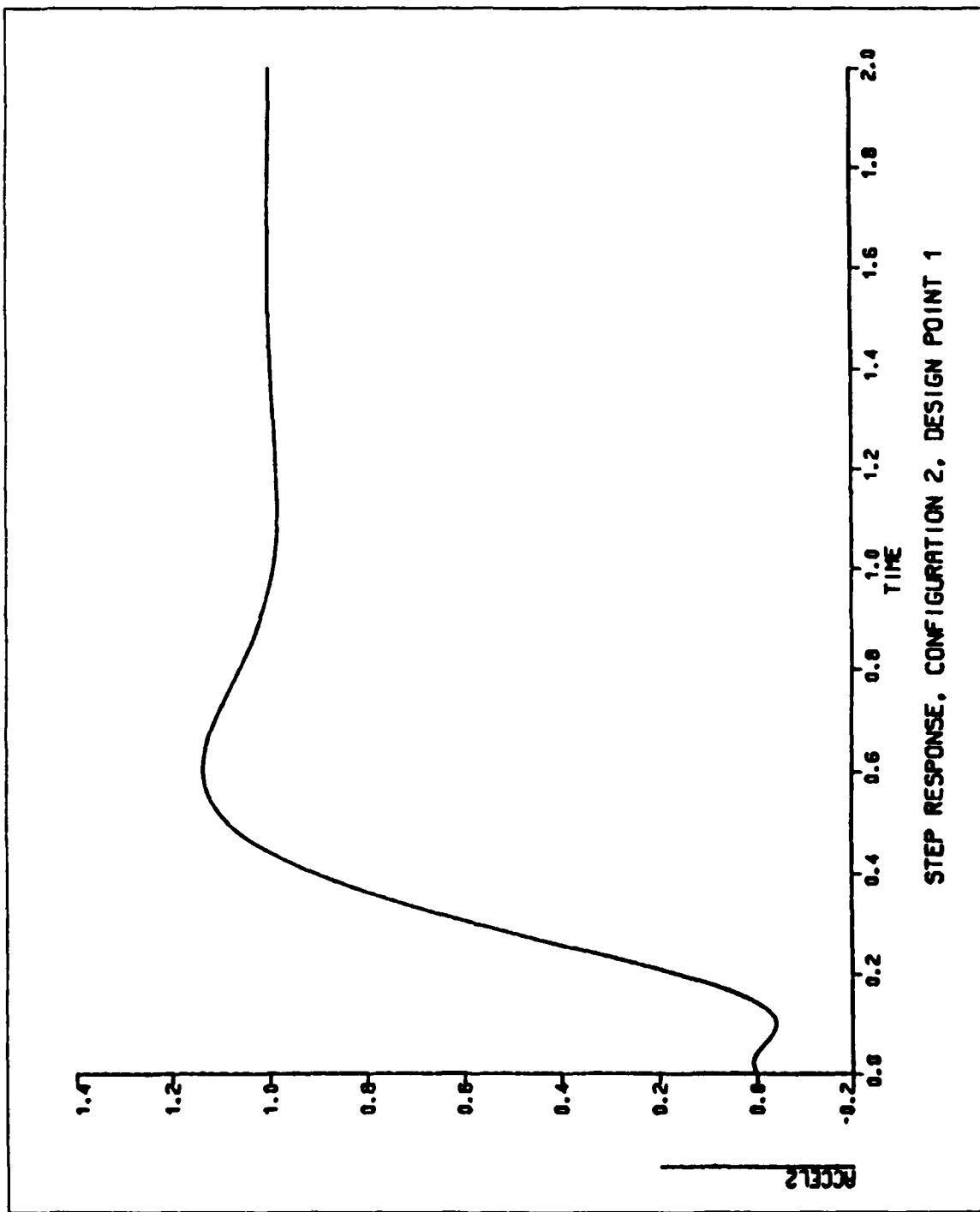
Figure 12.   Step Response of Autopilot Configuration Two at Design Point One
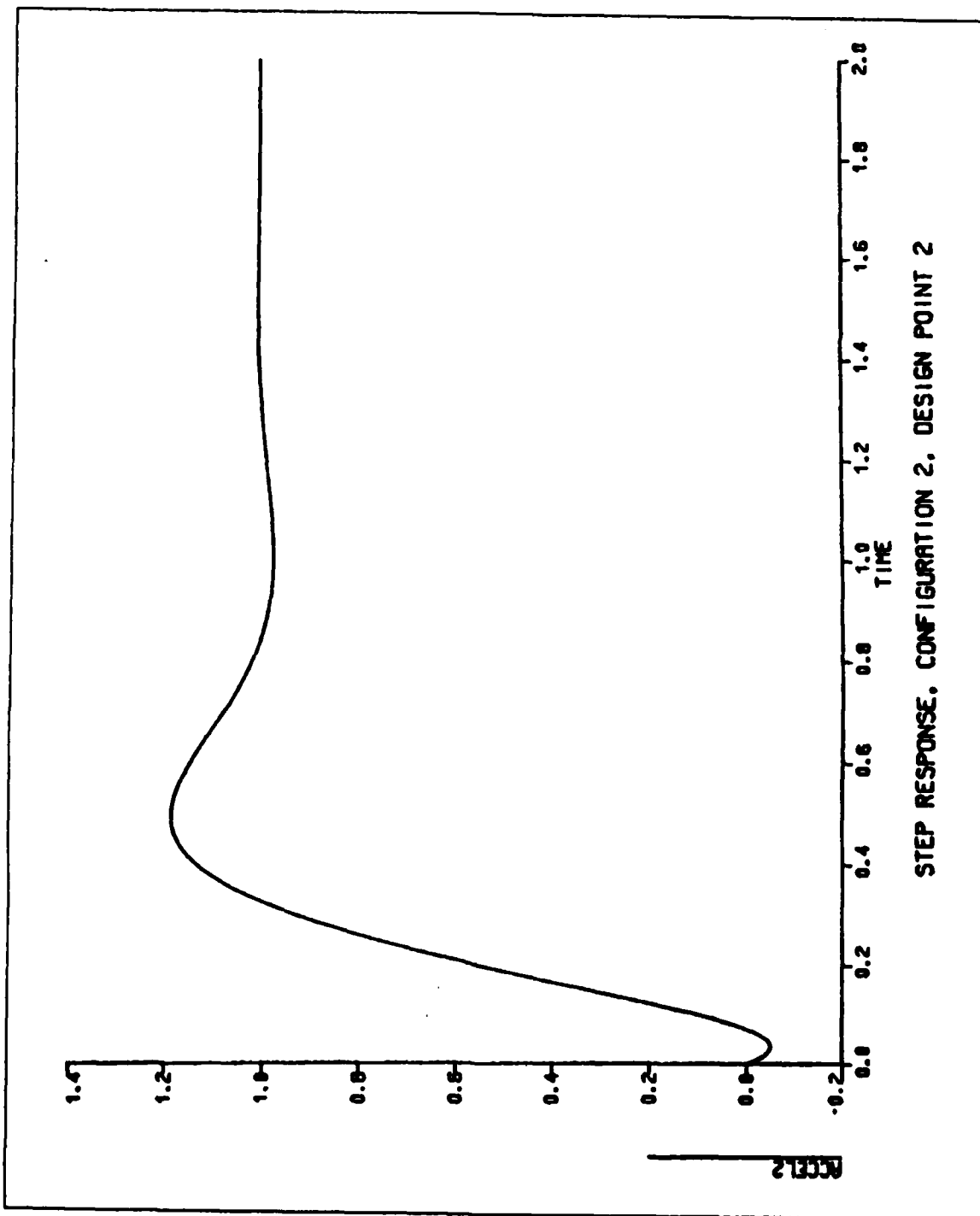
Figure 13.   Step Response of Autopilot Configuration Two at Design Point Two
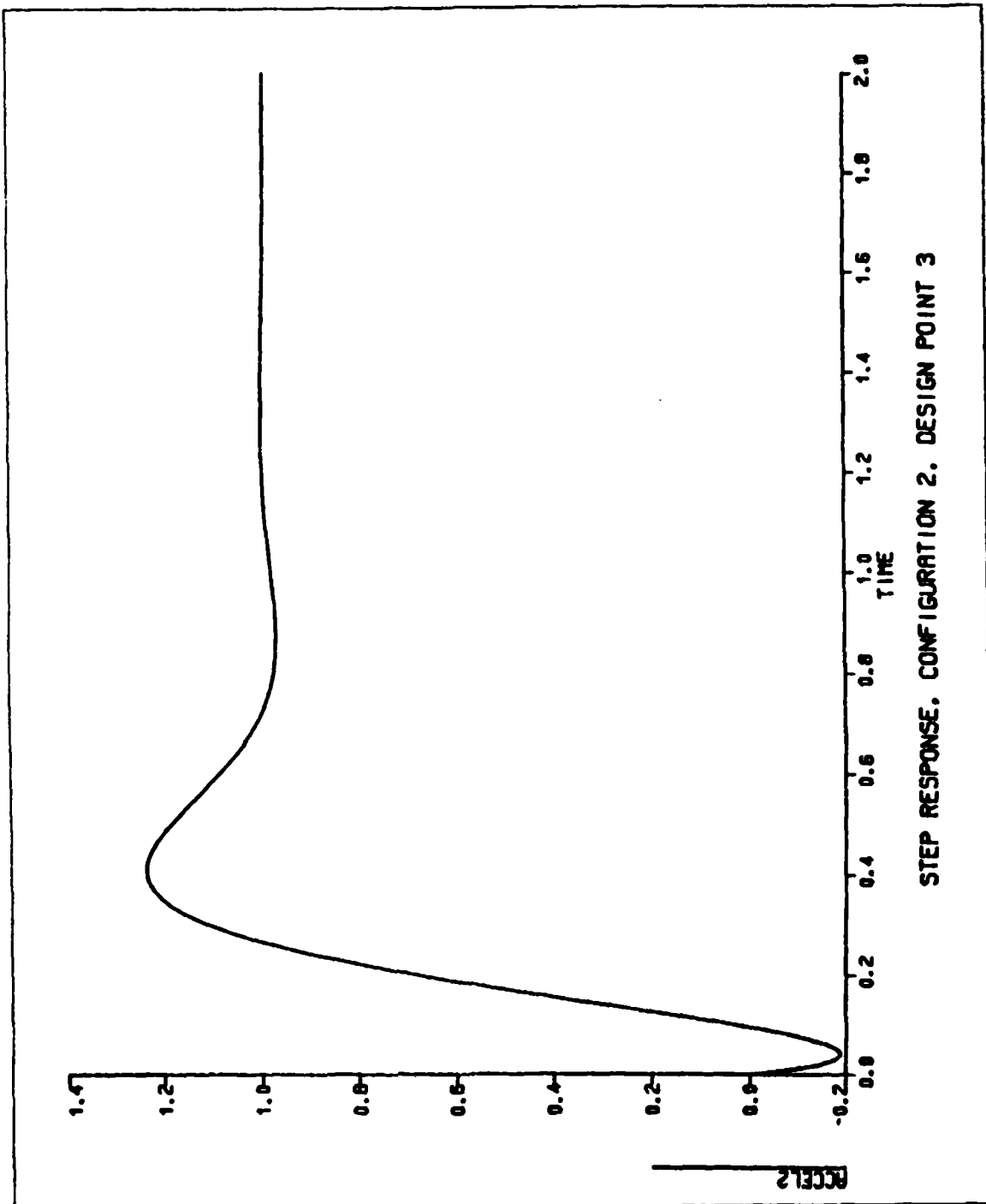
Figure 14.   Step Response of Autopilot Configuration Two at Design Point Three
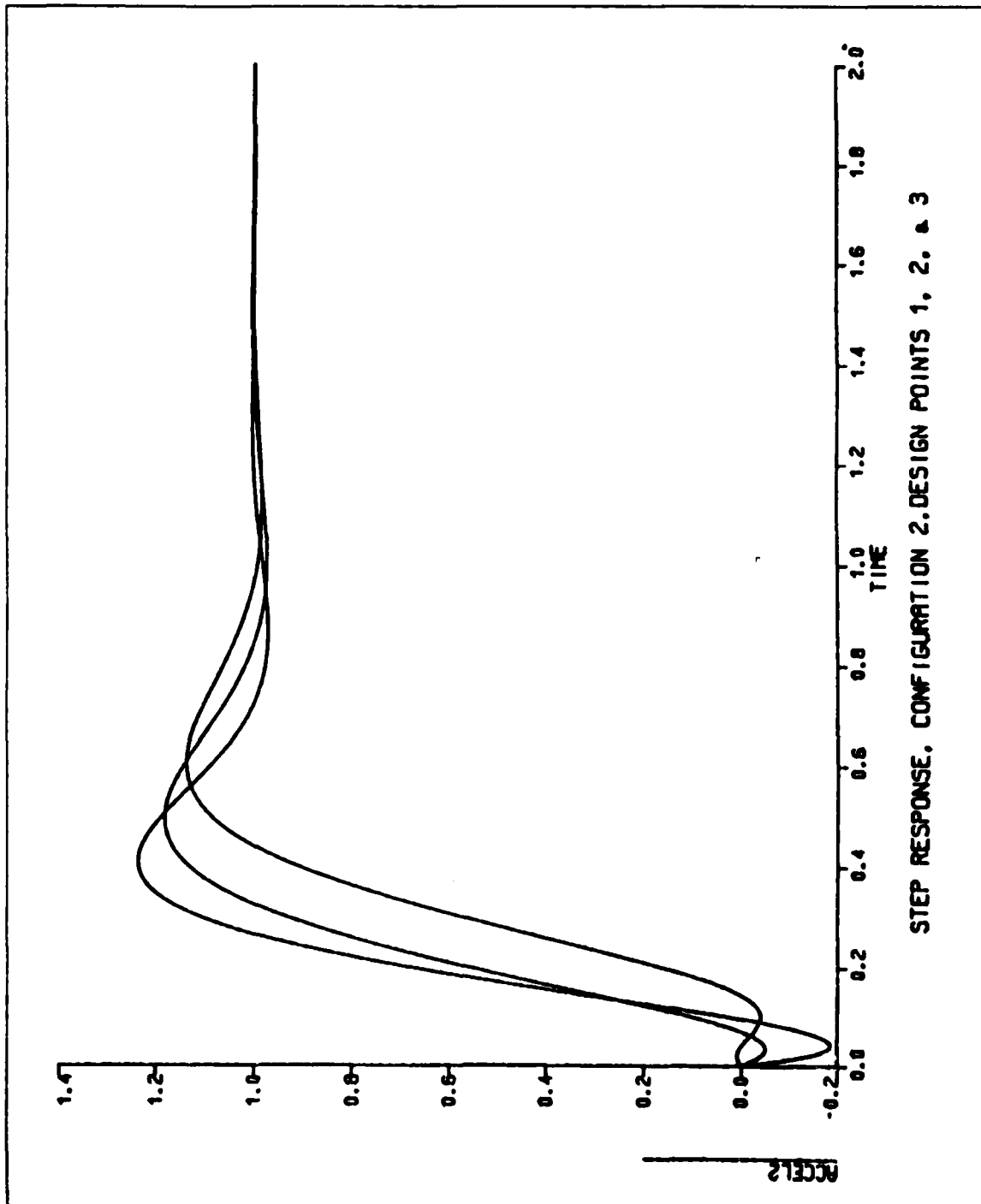
Figure 15. Parametric Comparison of the Step Response of Autopilot Configuration Two at Three Design Points
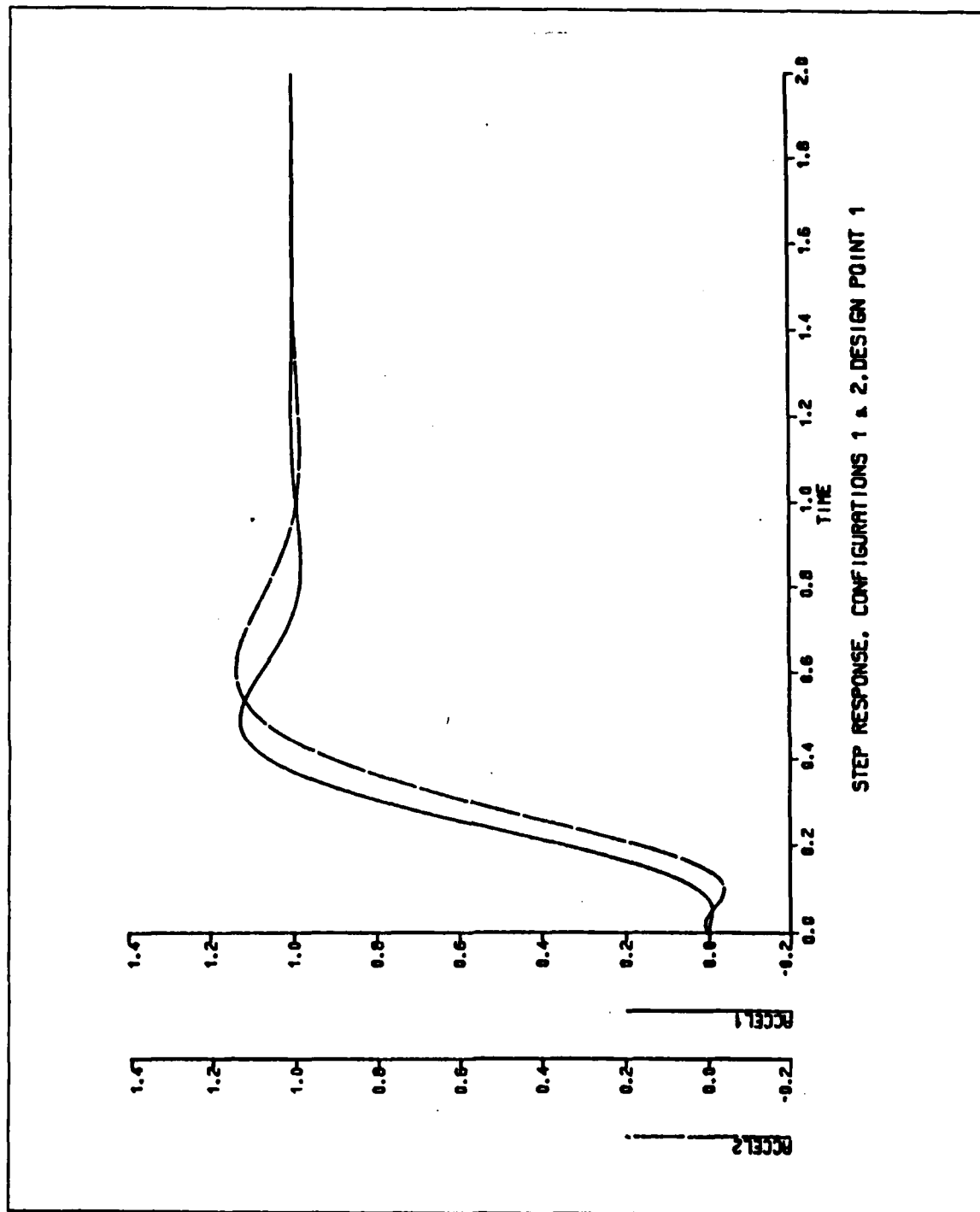
Figure 16.   Parametric Comparison of the Step Response of Autopilot Configurations One and Two at Design Point One
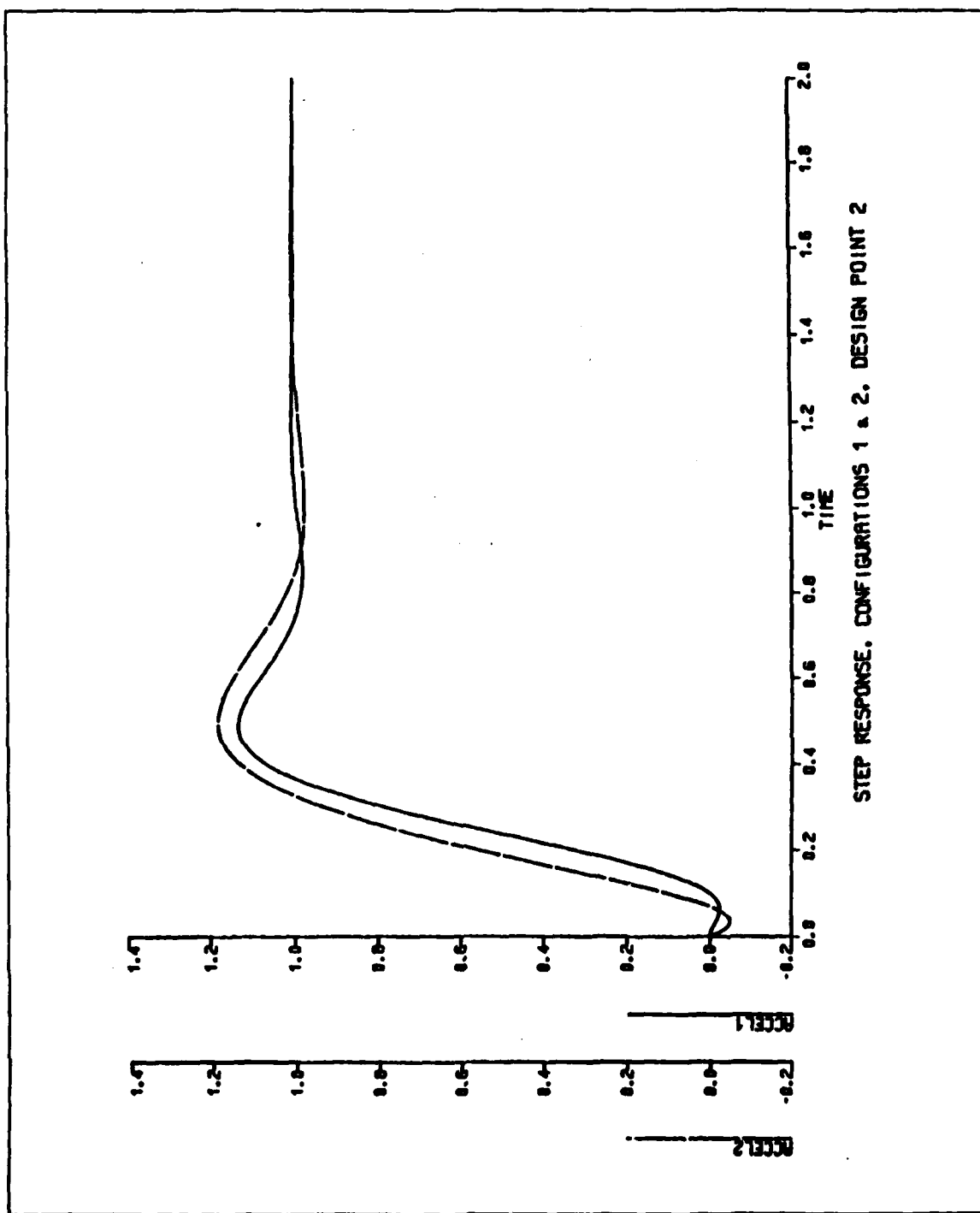
Figure 17. Parametric Comparison of the Step Response of Autopilot Configurations One and Two at Design Point Two
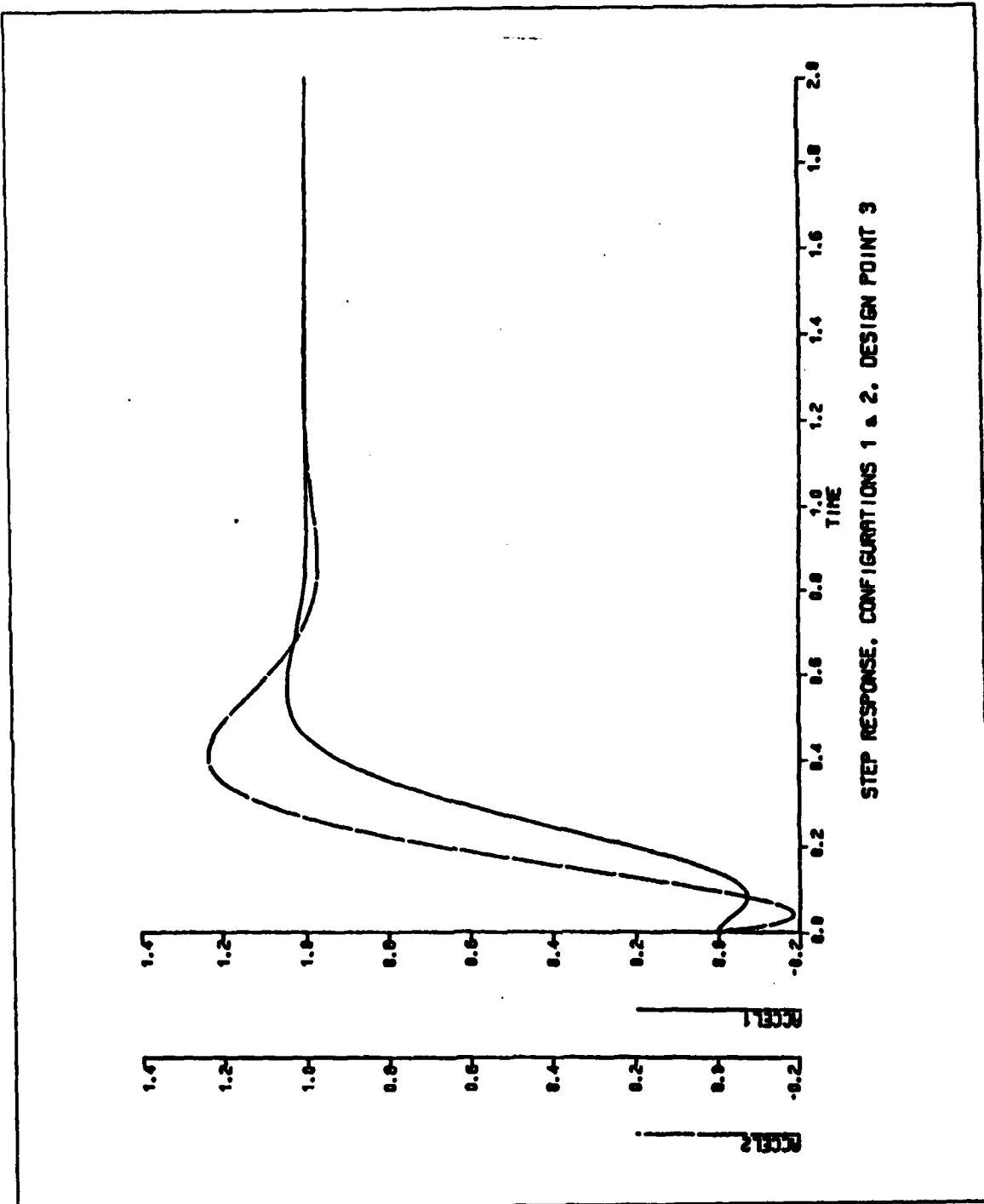
Figure 18. Parametric Comparison of the Step Response of Autopilot Configurations One and Two at Design Point Three

B. ANALYSIS OF SIMULATION RESULTS

In the analysis of the simulation results, there are two characteristics of the step response which are of interest. They are the rise time, t_r, and the settling time, t_s.

The rise time is simply defined as the time required for the systems output response to go from 10 percent to 90 percent of its final value. This can be measured directly off of the graphical simulation results. [Ref. 9: p. 40]

· The settling time, t_s, is defined as four time constants, or

$$t_s = \frac{4}{\zeta \omega_n}. \tag{4.1}$$

The value of the maximum overshoot, M_{pt}, and the time at which the maximum overshoot occurs, t_p, can be measured directly off the graphical output. The maximum overshoot is defined as

$$M_{pt} = 1 + \exp\left(\frac{-\pi \zeta}{\sqrt{1 - \zeta^2}}\right) \tag{4.2}$$

and the time at which it occurs

$$t_p = \frac{\pi}{\omega_n \sqrt{1 - \zeta^2}}. \tag{4.3}$$

Measurements of M_{pt} and t_p are made from the graphical output of Figure 8 on page 23 through Figure 10 on page 25 for Configuration One and from Figure 12 on page 27 through Figure 14 on page 29 for Configuration Two. Once M_{pt} and t_p are measured, ζ and ω_n are obtained by solving simultaneously Equations (4.2) and (4.3). The values for ζ and ω_n are then used in Equation (4.1) to obtain the settling time, t_s. The response characteristics M_{pt}, t_p, ζ, ω_n, t_s and t_r are tabulated in Table 8 and Table 9 on page 35. [Ref. 5: pp. 108-109]

Table 8. RESPONSE CHARACTERISTICS FOR AUTOPILOT CONFIGURATION ONE

	DESIGN POINT 1	DESIGN POINT 2	DESIGN POINT 3
M_{pt}	1.12	1.13	1.07
t_p	0.51 sec	0.51 sec	0.57 sec
ζ	0.56	0.54	0.65
ω_n	7.47 rad/sec	7.36 rad/sec	7.24 rad/sec
t_s	0.96 sec	1.01 sec	0.85 sec
t_r	0.21 sec	0.19 sec	0.23 sec

Table 9. RESPONSE CHARACTERISTICS FOR AUTOPILOT CONFIGURATION TWO

	DESIGN POINT 1	DESIGN POINT 2	DESIGN POINT 3
M_{pt}	1.13	1.19	1.24
t_p	0.63 sec	0.52 sec	0.43 sec
ζ	0.54	0.47	0.41
ω_n	5.95 rad/sec	6.84 rad/sec	8.03 rad/sec
t_s	1.24 sec	1.24 sec	1.20 sec
t_r	0.23 sec	0.19 sec	0.14 sec

35

V. CONCLUSIONS

The step responses of the two autopilot configurations were compared at three different design points. Both configurations met the desired response specifications of $\zeta \simeq 0.5$ and $\omega_n \simeq 10$. The actual values of ζ and ω_n are given in Table 8 and Table 9 on page 35 for Configurations One and Two respectively.

At Design Point One, Configuration One's observed rise time is nine percent less than that of Configuration Two, and Configuration One's observed settling time is twenty-three percent less than that of Configuration Two. The two configurations are compared graphically in Figure 16 on page 31.

At Design Point Two, Configuration One's observed rise time is equal to that of Configuration Two, and Configuration One's observed settling time is nineteen percent less than that of Configuration Two. The graphical comparison is shown in Figure 17 on page 32.

At Design Point Three, Configuration One's observed rise time is sixty-four percent more than that of Configuration Two, and Configuration One's observed settling time is thirty percent less than that of Configuration Two. This comparison is shown graphically in Figure 18 on page 33.

The apparent trend is that Configuration One's rise time increases slightly as the flight of the missile continues but that its settling time decreases slightly. This trend is graphically depicted in Figure 11 on page 26. Configuration Two's rise time decreases significantly as the flight of the missile continues but its settling time remains nearly constant. This trend is shown graphically in Figure 15 on page 30.

The shorter rise time, later in flight, of Configuration Two, is viewed as a significant performance advantage over Configuration One. It is clear that a shorter rise time means a faster response. This faster response is desirable late in flight because it is during this later part of the missile's flight that the missile would be in its final phase of closing on and tracking a maneuvering target. For this reason, faster response, later in flight, is a significant advantage.

APPENDIX A. ORIGINAL WIND TUNNEL DATA

Table 10. AXIAL FORCE COEFFICIENTS (POWER ON)

ALT (KM) (km)	ALPHA (degrees)	MACH 2.60	MACH 3.20	MACH 3.80
0	0	0.324	0.288	0.258
	3.0	0.326	0.289	0.260
	5.0	0.328	0.292	0.263
	10.0	0.338	0.305	0.278
	20.0	0.358	0.336	0.322
	30.0	0.248	0.323	0.422
8	0	0.334	0.295	0.263
	3.0	0.335	0.296	0.265
	5.0	0.338	0.299	0.268
	10.0	0.348	0.312	0.283
	20.0	0.367	0.343	0.328
	30.0	0.257	0.330	0.427
16	0	0.353	0.311	0.278
	3.0	0.355	0.313	0.279
	5.0	0.357	0.316	0.282
	10.0	0.367	0.329	0.297
	20.0	0.387	0.360	0.342
	30.0	0.276	0.347	0.441
24	0	0.381	0.336	0.299
	3.0	0.383	0.337	0.301
	5.0	0.385	0.340	0.304
	10.0	0.395	0.353	0.319
	20.0	0.415	0.384	0.363
	30.0	0.304	0.371	0.462

Table 11. **AXIAL FORCE COEFFICIENTS (POWER OFF)**

ALT (km)	ALPHA (degrees)	MACH 2.60	MACH 3.20	MACH 3.80
0	0	0.392	0.342	0.303
	3.0	0.394	0.344	0.305
	5.0	0.396	0.347	0.308
	10.0	0.407	0.360	0.323
	20.0	0.429	0.391	0.367
	30.0	0.321	0.378	0.466
8	0	0.401	0.349	0.308
	3.0	0.403	0.351	0.310
	5.0	0.406	0.354	0.313
	10.0	0.416	0.367	0.328
	20.0	0.438	0.398	0.372
	30.0	0.331	0.385	0.471
16	0	0.421	0.366	0.322
	3.0	0.422	0.368	0.324
	5.0	0.425	0.370	0.327
	10.0	0.436	0.383	0.342
	20.0	0.458	0.414	0.387
	30.0	0.350	0.401	0.486
24	0	0.449	0.390	0.344
	3.0	0.451	0.392	0.345
	5.0	0.453	0.395	0.348
	10.0	0.464	0.408	0.363
	20.0	0.486	0.438	0.408
	30.0	0.378	0.425	0.507

Table 12. NORMAL FORCE COEFFICIENTS

DELTA (degrees)	ALPHA (degrees)	MACH 2.60	MACH 3.20	MACH 3.80
-30	0	-1.104	-0.999	-0.525
	3.0	-0.459	-0.392	-0.015
	5.0	-0.047	0.013	0.353
	10.0	1.336	1.363	1.594
	20.0	5.004	4.877	4.739
	30.0	9.420	8.992	8.391
-20	0	-0.802	-0.660	-0.423
	3.0	-0.138	-0.041	0.102
	5.0	0.291	0.368	0.479
	10.0	1.699	1.707	1.743
	20.0	5.358	5.163	4.926
	30.0	9.758	9.259	8.604
-10	0	-0.385	-0.305	-0.236
	3.0	0.272	0.294	0.300
	5.0	0.689	0.692	0.683
	10.0	2.076	2.008	1.959
	20.0	5.723	5.451	5.159
	30.0	10.156	9.577	8.839
0	0	0.000	0.000	0.000
	3.0	0.652	0.594	0.539
	5.0	1.067	0.989	0.923
	10.0	2.457	2.309	2.201
	20.0	6.142	5.788	5.391
	30.0	10.625	10.004	9.043
10	0	0.385	0.305	0.236
	3.0	1.046	0.908	0.770
	5.0	1.469	1.312	1.151
	10.0	2.888	2.660	2.471
	20.0	6.585	6.225	5.572
	30.0	11.014	10.421	9.175
20	0	0.802	0.660	0.423
	3.0	1.460	1.286	0.946
	5.0	1.879	1.709	1.319
	10.0	3.271	3.063	2.563
	20.0	6.911	6.574	5.667
	30.0	11.264	10.731	9.208
30	0	1.104	0.999	0.525
	3.0	1.747	1.606	1.033
	5.0	2.154	2.009	1.396
	10.0	3.513	3.342	2.613
	20.0	7.072	6.804	5.659
	30.0	11.430	10.889	9.141

Table 13. PITCHING MOMENT COEFFICIENTS

DELTA (degrees)	ALPHA (degrees)	MACH 2.60	MACH 3.20	MACH 3.80
-30	0	7.313	6.609	3.437
	3.0	7.308	6.480	3.601
	5.0	7.016	6.148	3.451
	10.0	6.632	5.432	3.254
	20.0	6.353	4.212	2.740
	30.0	2.980	0.503	1.222
-20	0	5.307	4.366	2.797
	3.0	5.185	4.161	2.828
	5.0	4.782	3.802	2.616
	10.0	4.227	3.152	2.272
	20.0	4.013	2.317	1.508
	30.0	0.745	-1.259	-0.188
-10	0	2.550	2.017	1.560
	3.0	2.469	1.944	1.524
	5.0	2.146	1.662	1.271
	10.0	1.735	1.160	0.839
	20.0	1.592	0.414	-0.034
	30.0	-1.889	-3.362	-1.736
0	0	0.000	0.000	0.000
	3.0	-0.043	-0.034	-0.054
	5.0	-0.355	-0.303	-0.315
	10.0	-0.780	-0.818	-0.749
	20.0	-1.167	-1.805	-1.553
	30.0	-5.033	-6.229	-3.093
10	0	-2.550	-2.017	-1.560
	3.0	-2.655	-2.115	-1.586
	5.0	-3.023	-2.441	-1.824
	10.0	-3.646	-3.150	-2.184
	20.0	-4.113	-4.706	-2.764
	30.0	-7.570	-8.942	-3.960
20	0	-5.307	-4.366	-2.797
	3.0	-5.398	-4.618	-2.750
	5.0	-5.735	-5.067	-2.935
	10.0	-6.182	-5.816	-3.149
	20.0	-6.269	-7.017	-3.388
	30.0	-9.224	-10.995	-4.178
30	0	-7.313	-6.609	-3.473
	3.0	-7.297	-6.732	-3.326
	5.0	-7.556	-7.054	-3.442
	10.0	-7.784	-7.664	-3.479
	20.0	-7.338	-8.535	-3.339
	30.0	-10.323	-12.038	-3.732

APPENDIX B. INTERPOLATED WIND TUNNEL DATA

Table 14. AXIAL FORCE COEFFICIENTS (POWER ON)

ALPHA (degrees)	DESIGN POINT 1	DESIGN POINT 2	DESIGN POINT 3
0	0.278	0.280	0.319
3.0	0.280	0.281	0.320
5.0	0.283	0.284	0.323
10.0	0.296	0.299	0.336
20.0	0.335	0.341	0.367
30.0	0.373	0.418	0.349

Table 15. AXIAL FORCE COEFFICIENTS (POWER OFF)

ALPHA (degrees)	DESIGN POINT 1	DESIGN POINT 2	DESIGN POINT 3
0	0.310	0.326	0.374
3.0	0.329	0.328	0.376
5.0	0.332	0.331	0.379
10.0	0.347	0.346	0.392
20.0	0.383	0.387	0.421
30.0	0.421	0.464	0.404

Table 16. NORMAL FORCE COEFFICIENTS

DELTA (degrees)	ALPHA (degrees)	DESIGN POINT 1	DESIGN POINT 2	DESIGN POINT 3
-30	0	-0.778	-0.620	-1.004
	3.0	-0.216	-0.090	-0.395
	5.0	0.332	0.285	0.010
	10.0	1.417	1.548	1.362
	20.0	4.813	4.767	4.883
	30.0	8.712	8.511	9.013
-20	0	-0.549	-0.470	-0.667
	3.0	0.026	0.073	-0.046
	5.0	0.420	0.456	0.364
	10.0	1.724	1.736	1.707
	20.0	5.052	4.973	5.173
	30.0	8.953	8.735	9.284
-10	0	-0.273	-0.250	-0.309
	3.0	0.297	0.299	0.293
	5.0	0.688	0.685	0.692
	10.0	1.985	1.969	2.011
	20.0	5.315	5.217	5.465
	30.0	9.233	8.987	9.606
0	0	0.000	0.000	0.000
	3.0	0.568	0.550	0.597
	5.0	0.958	0.936	0.993
	10.0	2.259	2.223	2.316
	20.0	5.603	5.470	5.806
	30.0	9.556	9.235	10.035
10	0	0.273	0.250	0.309
	3.0	0.844	0.798	0.915
	5.0	1.237	1.183	1.320
	10.0	2.547	2.466	2.671
	20.0	5.920	5.703	6.243
	30.0	9.839	9.424	10.451
20	0	0.549	0.470	0.668
	3.0	1.127	1.014	1.295
	5.0	1.527	1.397	1.718
	10.0	2.830	2.663	3.073
	20.0	6.151	5.848	6.591
	30.0	10.020	9.513	10.758
30	0	0.778	0.620	1.004
	3.0	1.339	1.148	1.613
	5.0	1.723	1.519	2.016
	10.0	3.002	2.759	3.351
	20.0	6.268	5.888	6.817
	30.0	10.073	9.491	10.916

Table 17. PITCHING MOMENT COEFFICIENTS

DELTA (degrees)	ALPHA (degrees)	DESIGN POINT 1	DESIGN POINT 2	DESIGN POINT 3
-30	0	5.145	4.100	6.644
	3.0	5.136	4.177	6.521
	5.0	4.889	3.990	6.191
	10.0	4.416	3.690	5.492
	20.0	3.525	3.036	4.319
	30.0	0.839	1.078	0.627
-20	0	3.634	3.111	4.413
	3.0	3.539	3.095	4.212
	5.0	3.248	2.853	3.851
	10.0	2.741	2.448	3.206
	20.0	1.939	1.670	2.402
	30.0	-0.759	-0.402	-1.159
-10	0	1.804	1.651	2.044
	3.0	1.748	1.608	1.970
	5.0	1.480	1.349	1.686
	10.0	1.010	0.903	1.189
	20.0	0.205	0.056	0.473
	30.0	-2.603	-2.061	-3.288
0	0	0.000	0.000	0.000
	3.0	-0.043	-0.050	-0.034
	5.0	-0.309	-0.313	-0.306
	10.0	-0.786	-0.763	-0.816
	20.0	-1.687	-1.603	-1.773
	30.0	-4.765	-3.720	-6.169
10	0	-1.804	-1.651	-2.044
	3.0	-1.868	-1.692	-2.142
	5.0	-2.153	-1.947	-2.470
	10.0	-2.669	-2.377	-3.175
	20.0	-3.800	-3.152	-4.676
	30.0	-6.617	-4.956	-8.873
20	0	-3.634	-3.111	-4.413
	3.0	-3.746	-3.124	-4.657
	5.0	-4.072	-3.361	-5.100
	10.0	-4.571	-3.680	-5.834
	20.0	-5.323	-4.050	-6.980
	30.0	-7.814	-5.541	-10.906
30	0	-5.145	-4.100	-6.644
	3.0	-5.142	-4.007	-6.760
	5.0	-5.368	-4.164	-7.079
	10.0	-5.711	-4.316	-7.670
	20.0	-6.110	-4.378	-8.475
	30.0	-8.162	-5.393	-11.952

APPENDIX C.   LIFT AND DRAG COEFFICIENT DATA

Table 18.   LIFT COEFFICIENTS (POWER ON)

DELTA (degrees)	ALPHA (degrees)	DESIGN POINT 1	DESIGN POINT 2	DESIGN POINT 3
-30	0	-0.778	-0.620	-1.004
	3.0	-0.230	-0.105	-0.411
	5.0	0.306	0.259	-0.007
	10.0	1.397	1.473	1.283
	20.0	4.408	4.363	4.463
	30.0	7.358	7.162	7.631
-20	0	-0.549	-0.470	-0.668
	3.0	0.011	0.058	-0.063
	5.0	0.394	0.429	0.334
	10.0	1.646	1.658	1.623
	20.0	4.633	4.556	4.736
	30.0	7.567	7.356	7.866
-10	0	-0.273	-0.250	-0.309
	3.0	0.282	0.283	0.276
	5.0	0.661	0.658	0.661
	10.0	1.903	1.887	1.922
	20.0	4.880	4.786	5.010
	30.0	7.810	7.574	8.145
0	0	0.000	0.000	0.000
	3.0	0.553	0.535	0.579
	5.0	0.930	0.908	0.961
	10.0	2.173	2.137	2.222
	20.0	5.151	5.023	5.330
	30.0	8.089	7.789	8.516
10	0	0.273	0.250	0.309
	3.0	0.828	0.782	0.897
	5.0	1.208	1.154	1.287
	10.0	2.457	2.377	2.572
	20.0	5.448	5.242	5.741
	30.0	8.334	7.952	8.876
20	0	0.549	0.470	0.668
	3.0	1.111	0.998	1.276
	5.0	1.497	1.367	1.683
	10.0	2.736	2.571	2.968
	20.0	5.665	5.379	6.068
	30.0	8.491	8.030	9.142
30	0	0.778	0.620	1.004
	3.0	1.323	1.132	1.594
	5.0	1.692	1.488	1.980
	10.0	2.905	2.665	3.242
	20.0	5.775	5.416	6.280
	30.0	8.537	8.010	9.279

Table 19. LIFT COEFFICIENTS (POWER OFF)

DELTA (degrees)	ALPHA (degrees)	DESIGN POINT 1	DESIGN POINT 2	DESIGN POINT 3
-30	0	-0.778	-0.620	-1.004
	3.0	-0.233	-0.107	-0.414
	5.0	0.303	0.255	-0.023
	10.0	1.388	1.464	1.273
	20.0	4.392	4.347	4.445
	30.0	7.334	7.139	7.603
-20	0	-0.549	-0.470	-0.668
	3.0	0.009	0.056	-0.066
	5.0	0.389	0.425	0.330
	10.0	1.638	1.650	1.613
	20.0	4.616	4.541	4.717
	30.0	7.543	7.333	7.838
-10	0	-0.273	-0.250	-0.309
	3.0	0.279	0.281	0.273
	5.0	0.656	0.654	0.656
	10.0	1.895	1.879	1.912
	20.0	4.863	4.770	4.991
	30.0	7.786	7.551	8.117
0	0	0.000	0.000	0.000
	3.0	0.550	0.532	0.577
	5.0	0.925	0.904	0.956
	10.0	2.164	2.129	2.213
	20.0	5.134	5.008	5.312
	30.0	8.065	7.766	8.489
10	0	0.273	0.250	0.309
	3.0	0.8265	0.780	0.894
	5.0	1.203	1.150	1.282
	10.0	2.448	2.368	2.562
	20.0	5.432	5.227	5.723
	30.0	8.310	7.929	8.849
20	0	0.549	0.470	0.668
	3.0	1.108	0.995	1.274
	5.0	1.492	1.363	1.678
	10.0	2.727	2.562	2.958
	20.0	5.649	5.363	6.050
	30.0	8.467	8.0075	9.115
30	0	0.778	0.620	1.004
	3.0	1.327	1.129	1.591
	5.0	1.688	1.484	1.975
	10.0	2.896	2.657	3.232
	20.0	5.759	5.401	6.262
	30.0	8.513	7.987	9.252

Table 20.   DRAG COEFFICIENTS (POWER ON)

DELTA (degrees)	ALPHA (degrees)	DESIGN POINT 1	DESIGN POINT 2	DESIGN POINT 3
-30	0	0.278	0.280	0.319
	3.0	0.268	0.276	0.299
	5.0	0.311	0.308	0.323
	10.0	0.556	0.563	0.567
	20.0	1.196	1.951	2.015
	30.0	4.679	4.618	4.809
-20	0	0.278	0.280	0.319
	3.0	0.281	0.284	0.317
	5.0	0.319	0.323	0.353
	10.0	0.591	0.596	2.114
	20.0	2.043	2.021	4.944
	30.0	4.800	4.730	
-10	0	0.278	0.280	0.319
	3.0	0.295	0.296	0.335
	5.0	0.342	0.340	0.382
	10.0	0.636	0.636	0.680
	20.0	2.133	2.105	2.214
	30.0	4.940	4.856	5.105
0	0	0.278	0.280	0.319
	3.0	0.309	0.309	0.351
	5.0	0.365	0.364	0.408
	10.0	0.684	0.680	0.733
	20.0	2.231	2.191	2.331
	30.0	5.101	4.980	5.320
10	0	0.278	0.280	0.319
	3.0	0.324	0.322	0.367
	5.0	0.390	0.386	0.437
	10.0	0.734	0.723	0.795
	20.0	2.340	2.271	2.480
	30.0	5.243	5.074	5.528
20	0	0.278	0.280	0.319
	3.0	0.339	0.334	0.387
	5.0	0.415	0.405	0.472
	10.0	0.783	0.757	0.865
	20.0	2.419	2.321	2.599
	30.0	5.333	5.119	5.681
30	0	0.278	0.280	0.319
	3.0	0.350	0.341	0.404
	5.0	0.432	0.415	0.497
	10.0	0.813	0.774	0.913
	20.0	2.459	2.334	2.676
	30.0	5.360	5.108	5.760

Table 21. DRAG COEFFICIENTS (POWER OFF)

| DELTA (degrees)	ALPHA (degrees)	DESIGN POINT 1	DESIGN POINT 2	DESIGN POINT 3
-30	0	0.310	0.326	0.374
	3.0	0.317	0.323	0.355
	5.0	0.360	0.355	0.378
	10.0	0.597	0.610	0.623
	20.0	2.006	1.994	2.066
	30.0	4.721	4.657	4.856
-20	0	0.310	0.326	0.374
	3.0	0.330	0.331	0.373
	5.0	0.367	0.369	0.409
	10.0	0.641	0.642	0.682
	20.0	2.088	2.065	2.165
	30.0	4.841	4.769	4.992
-10	0	0.310	0.326	0.374
	3.0	0.344	0.343	0.391
	5.0	0.391	0.389	0.438
	10.0	0.686	0.683	0.735
	20.0	2.178	2.148	2.265
	30.0	4.981	4.895	5.153
0	0	0.310	0.326	0.374
	3.0	0.358	0.356	0.407
	5.0	0.414	0.411	0.464
	10.0	0.734	0.727	0.788
	20.0	2.276	2.235	2.381
	30.0	5.143	5.019	5.367
10	0	0.310	0.326	0.374
	3.0	0..373	0.369	0.423
	5.0	0.439	0.433	0.493
	10.0	0.784	0.769	0.850
	20.0	2.385	2.314	2.531
	30.0	5.284	5.114	5.575
20	0	0.310	0.326	0.374
	3.0	0.388	0.381	0.443
	5.0	0.464	0.451	0.527
	10.0	0.833	0.803	0.920
	20.0	2.464	2.364	2.650
	30.0	5.375	5.158	5.729
30	0	0.310	0.326	0.0374
	3.0	0.399	0.388	0.460
	5.0	0.481	0.462	0.553
	10.0	0.863	0.820	0.968
	20.0	2.504	2.377	2.727
	30.0	5.401	5.147	5.808

APPENDIX D. WIND TUNNEL GRAPHS
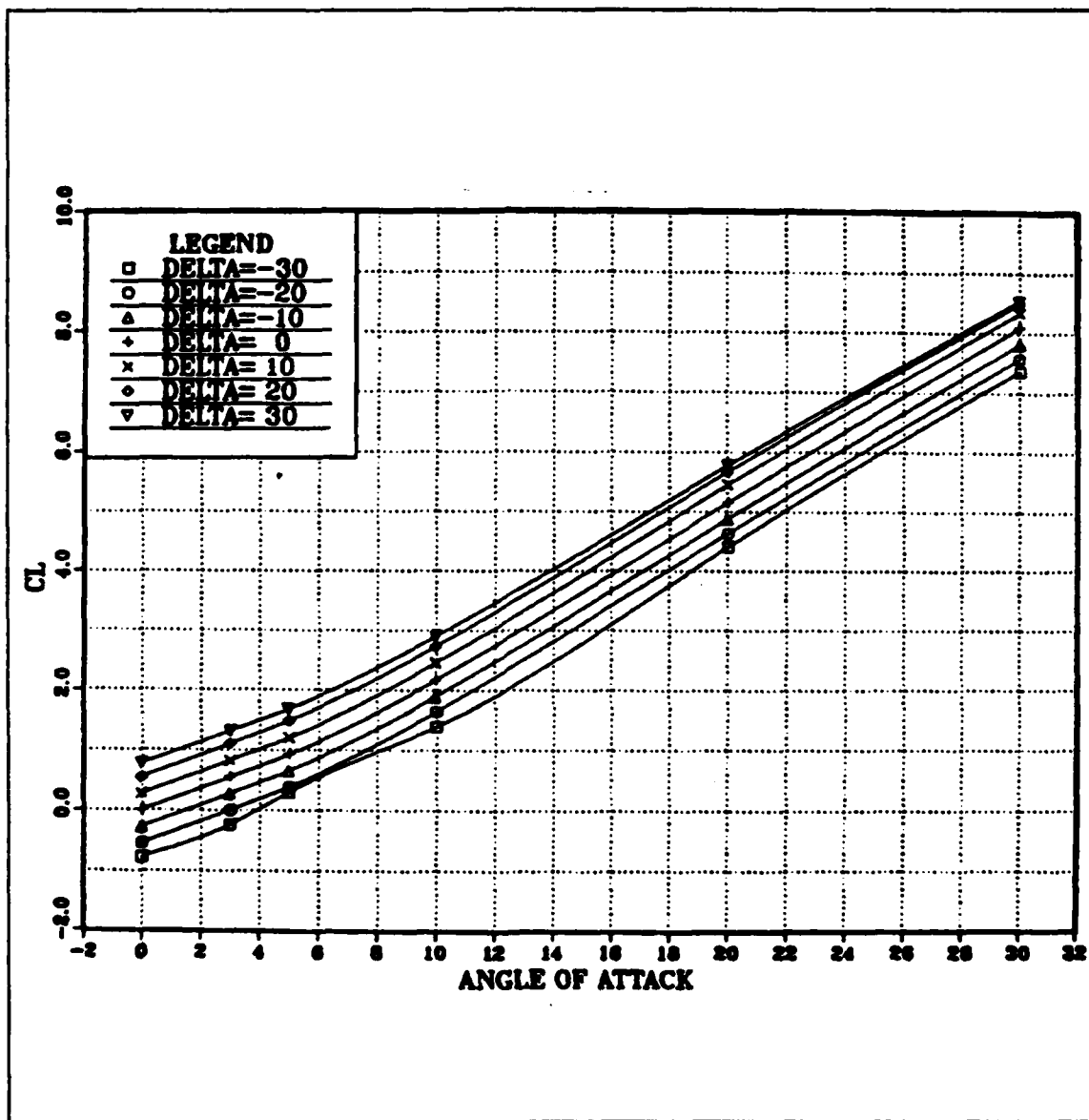
Figure 19.   Lift Coefficient versus Angle of Attack at Design Point One
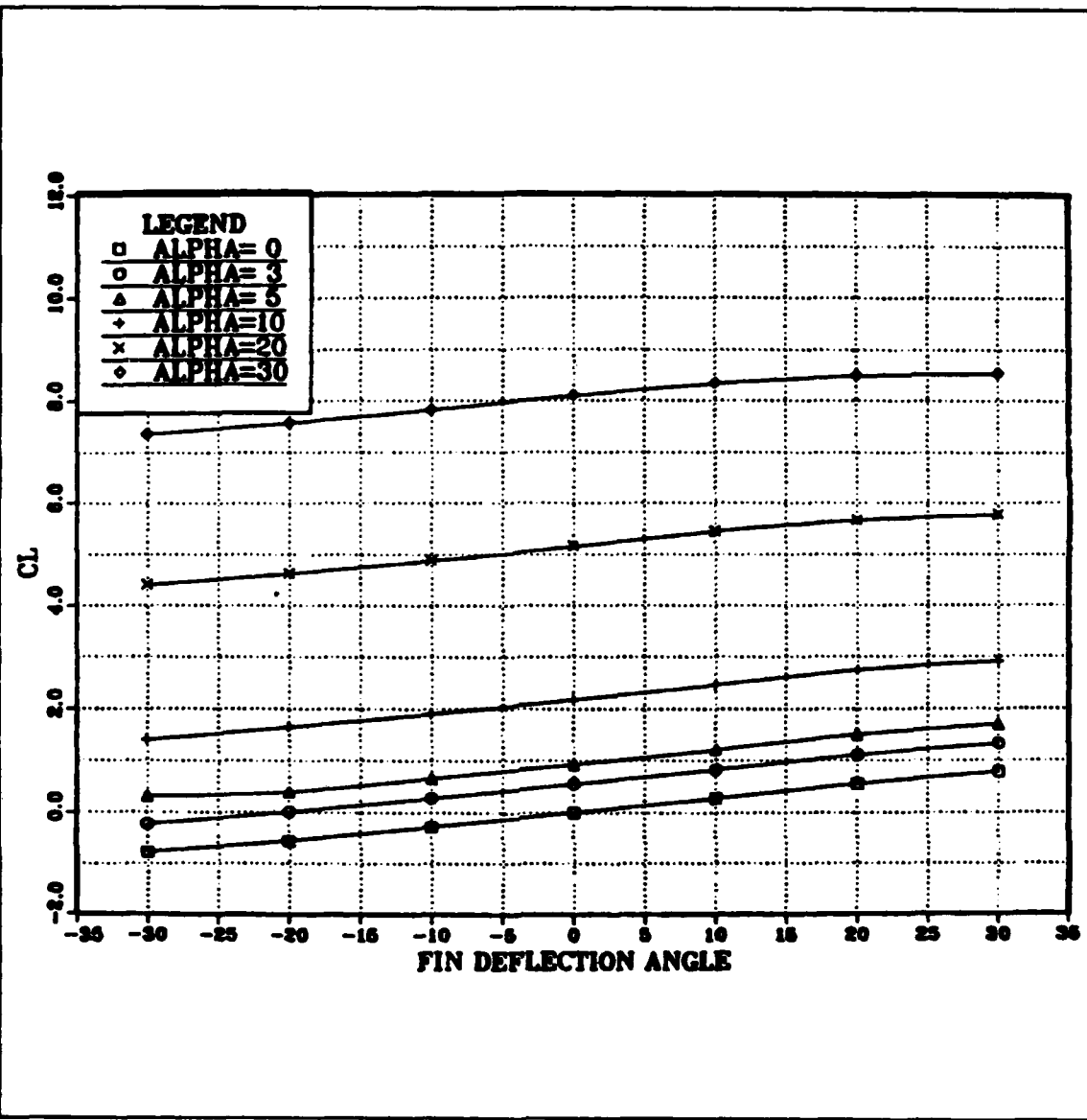
Figure 20.   Lift Coefficient versus Fin Deflection Angle at Design Point One
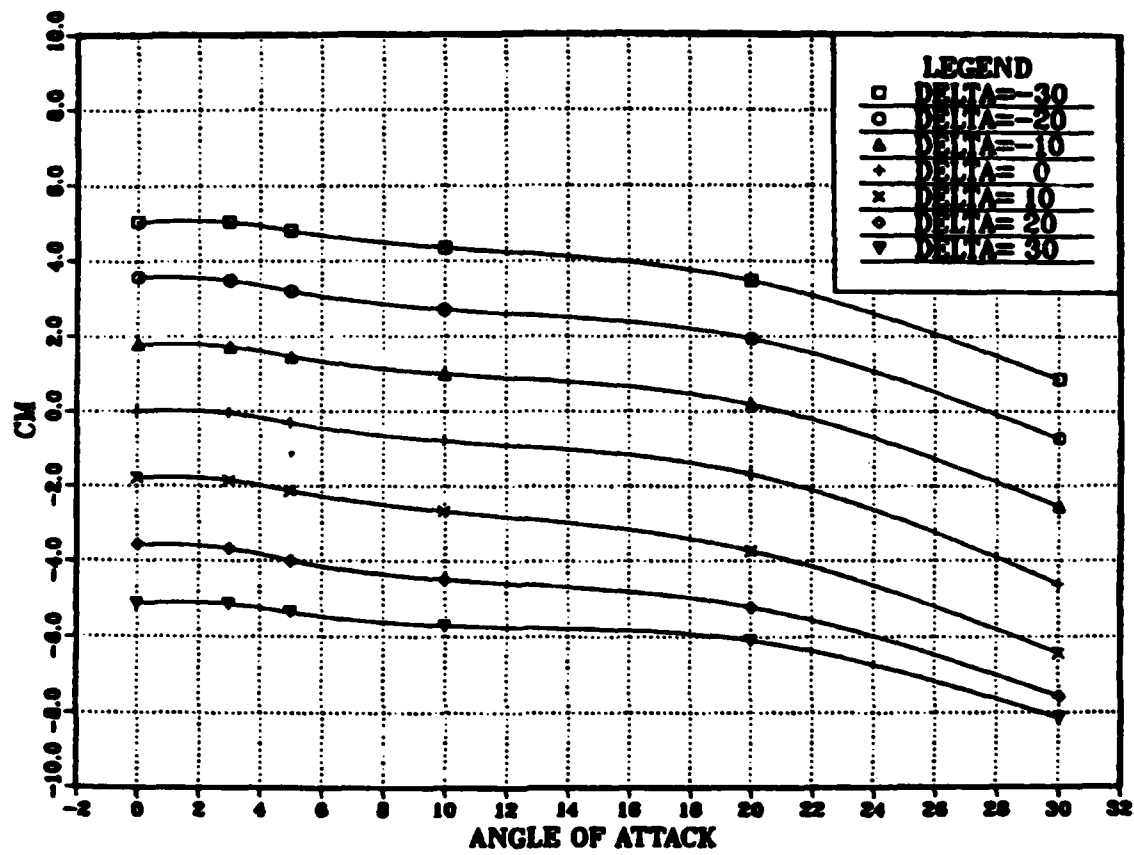
Figure 21.   Pitching Moment Coefficient versus Angle of Attack at Design Point
One
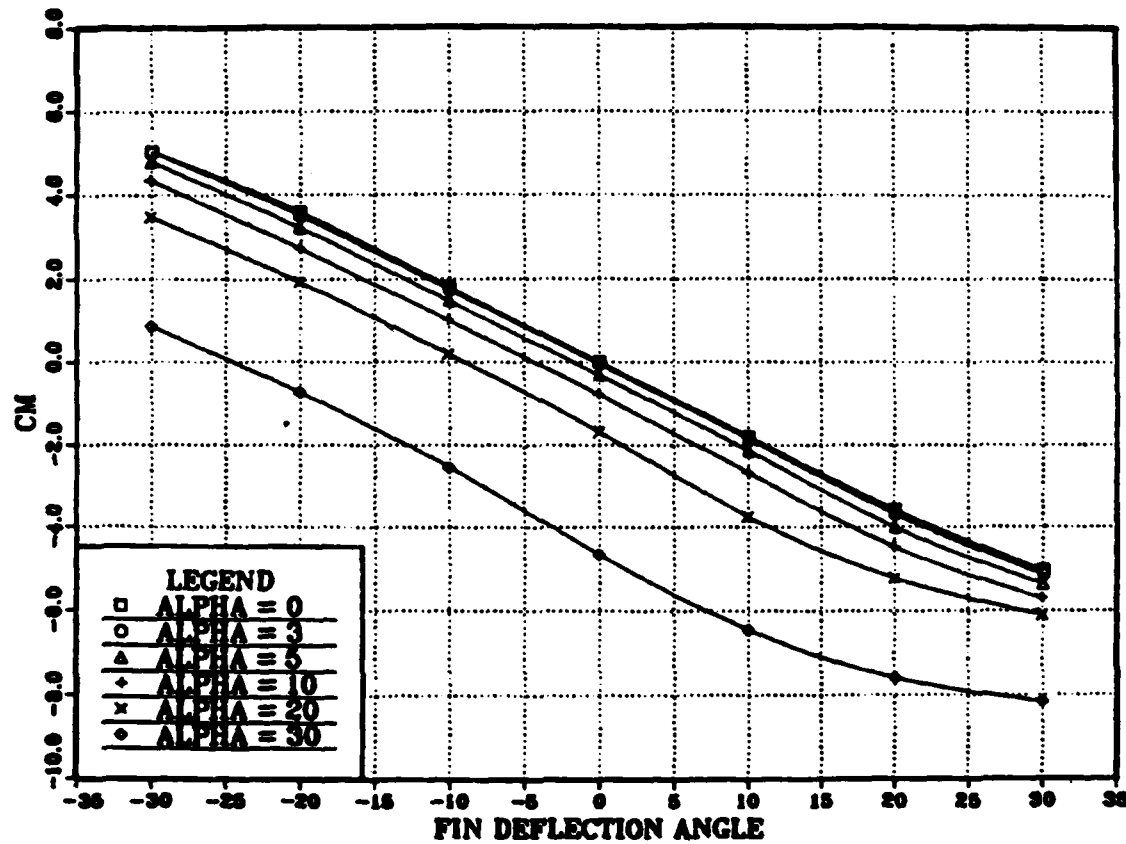
Figure 22.   Pitching Moment Coefficient versus Fin Deflection Angle at Design
Point One
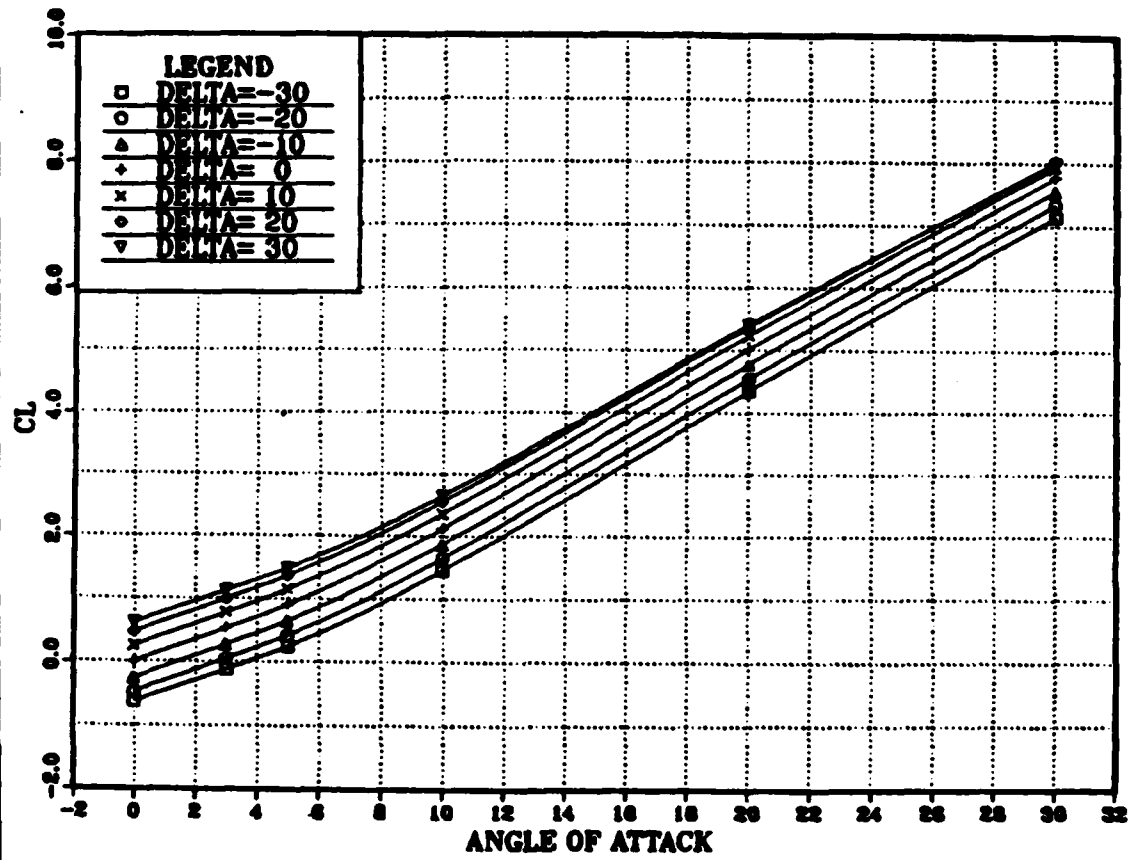
Figure 23.   Lift Coefficient versus Angle of Attack at Design Point Two
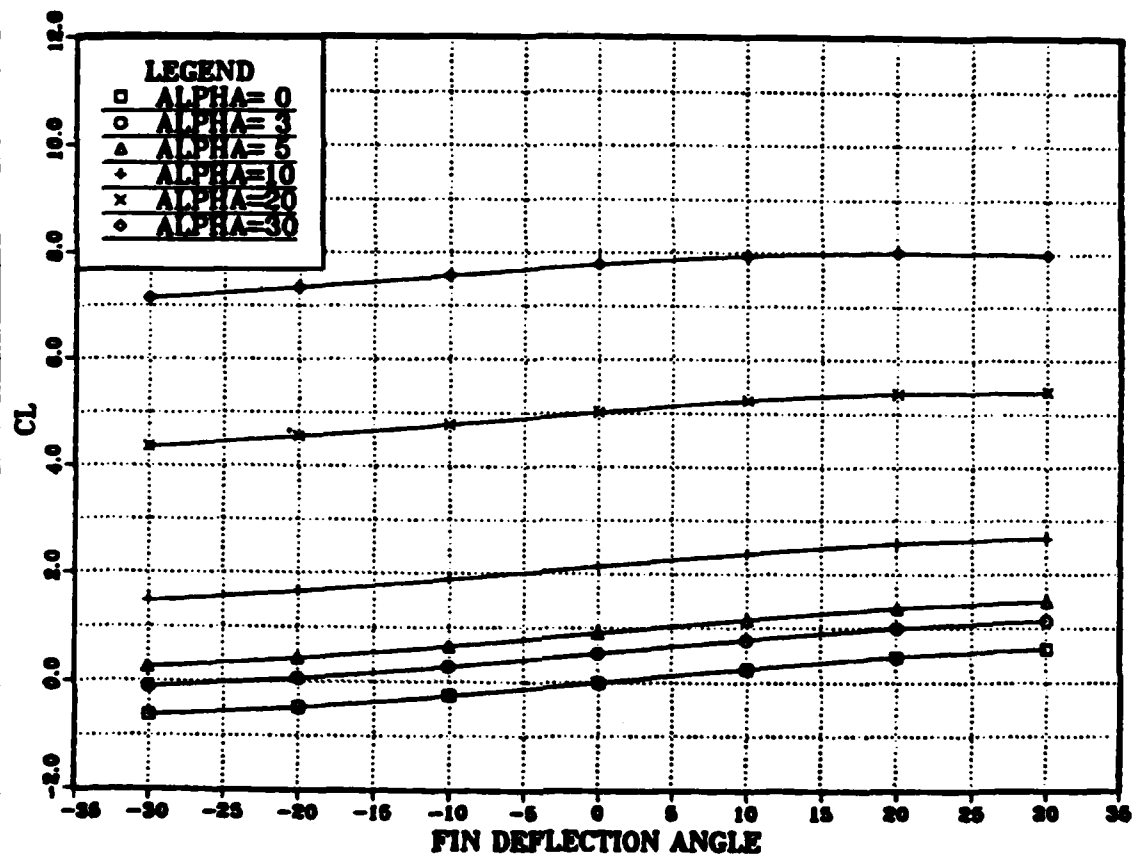
Figure 24.   Lift Coefficient versus Fin Deflection Angle at Design Point Two
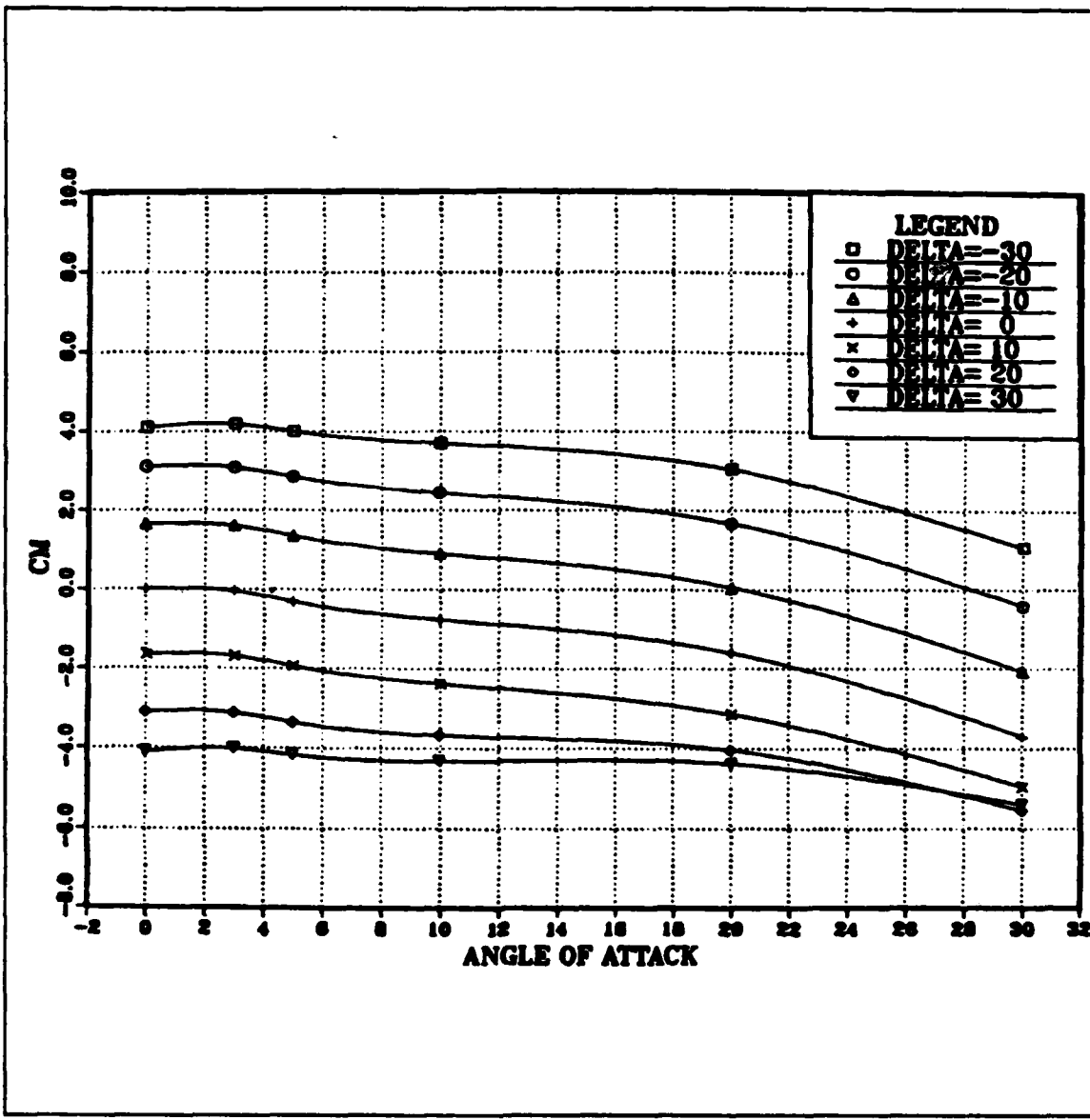
Figure 25. Pitching Moment Coefficient versus Angle of Attack at Design Point Two
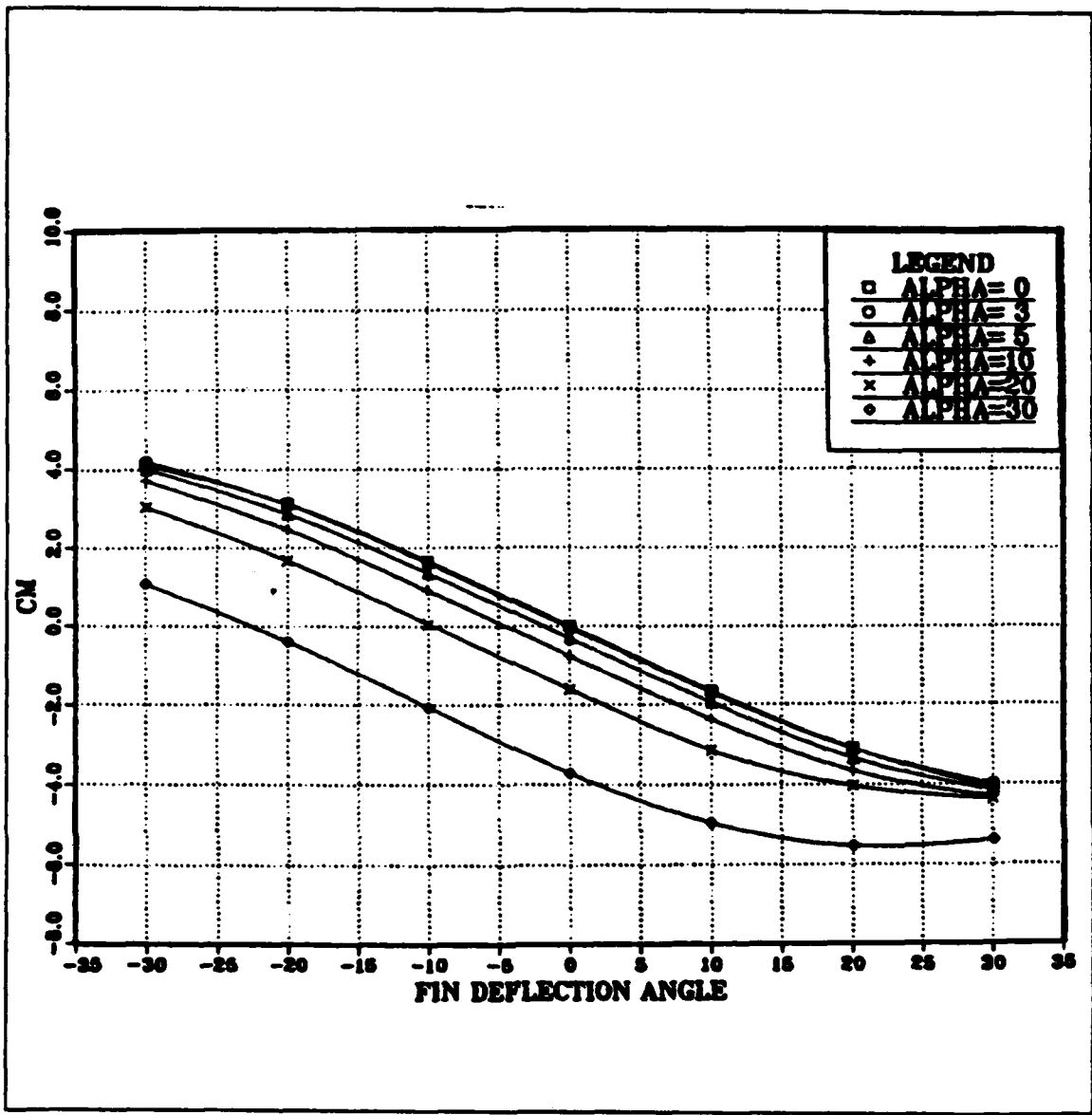
Figure 26. Pitching Moment Coefficient versus Fin Deflection Angle at Design Point Two
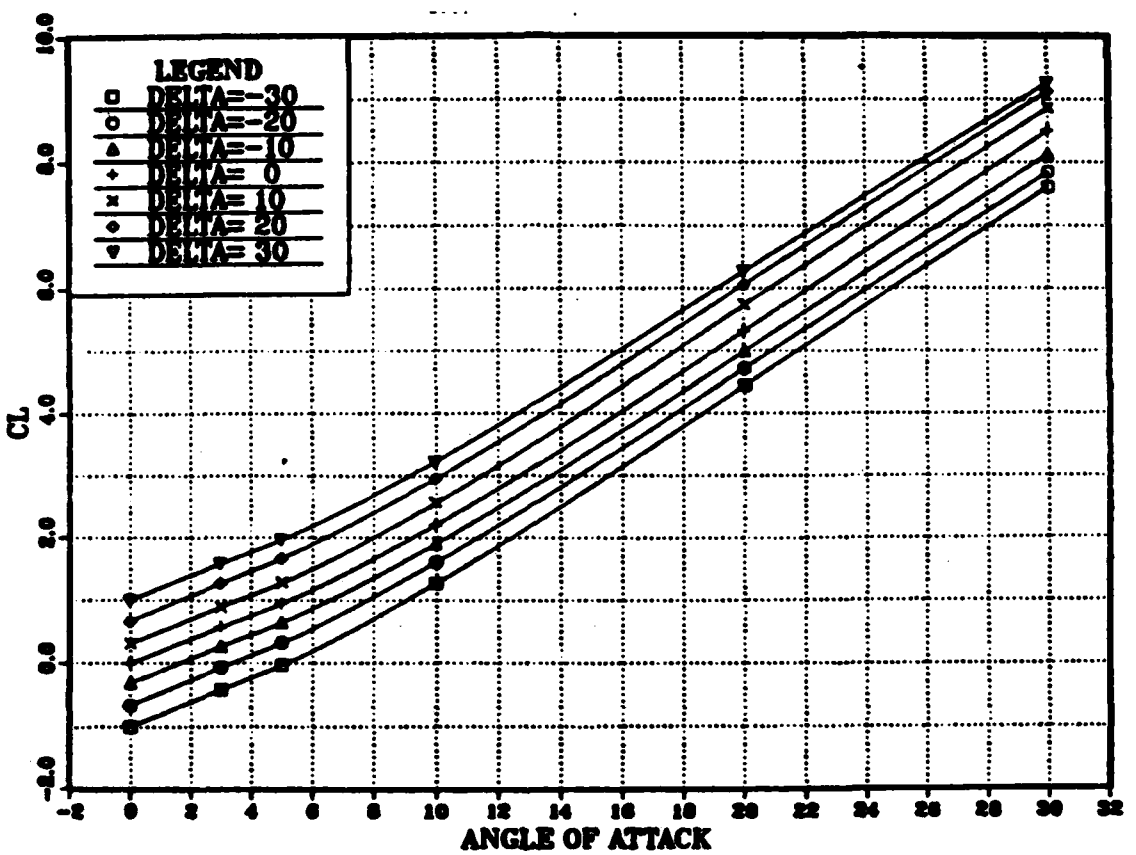
Figure 27.   Lift Coefficient versus Angle of Attack at Design Point Three
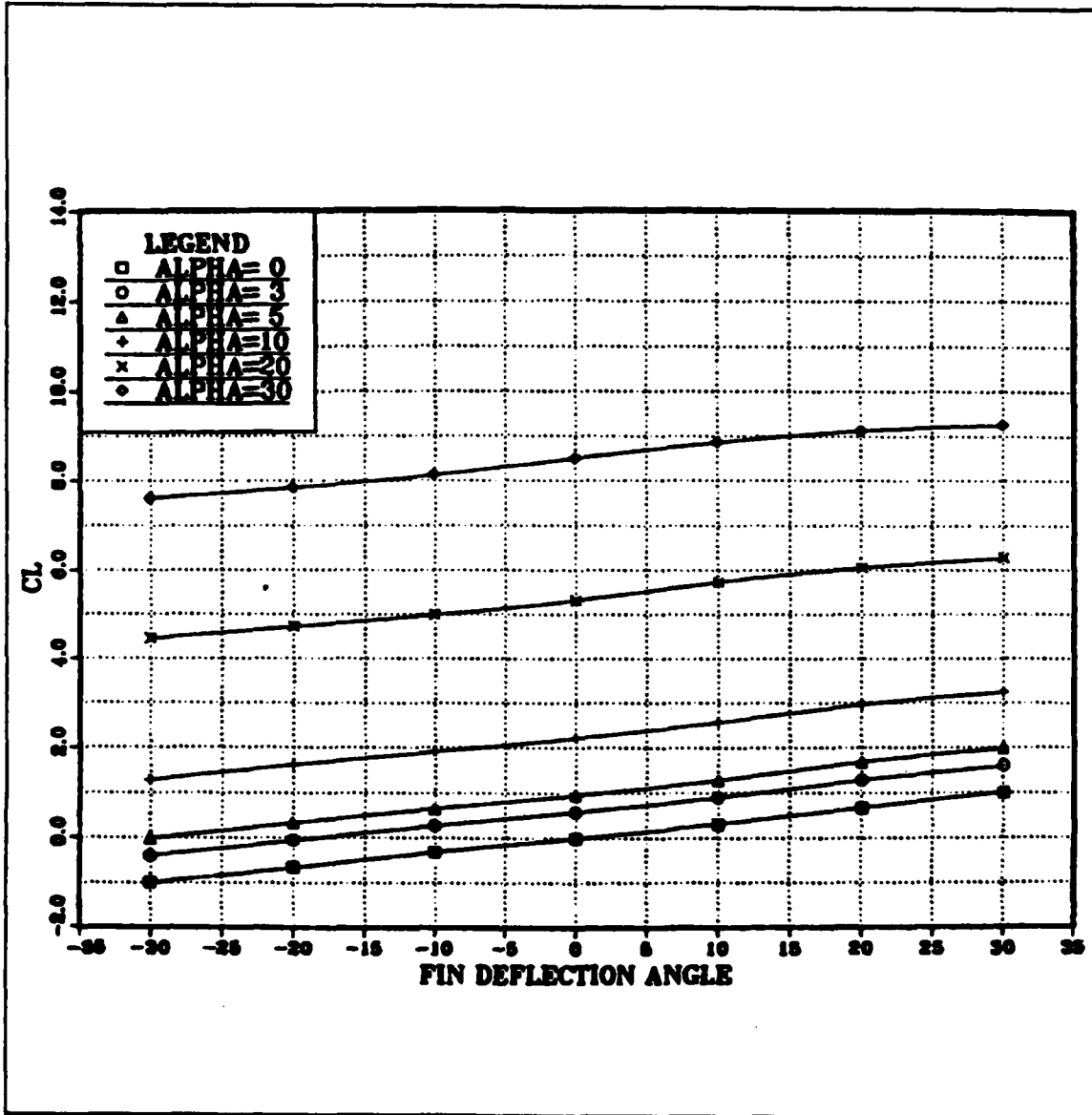
Figure 28.   Lift Coefficient versus Fin Deflection Angle at Design Point Three
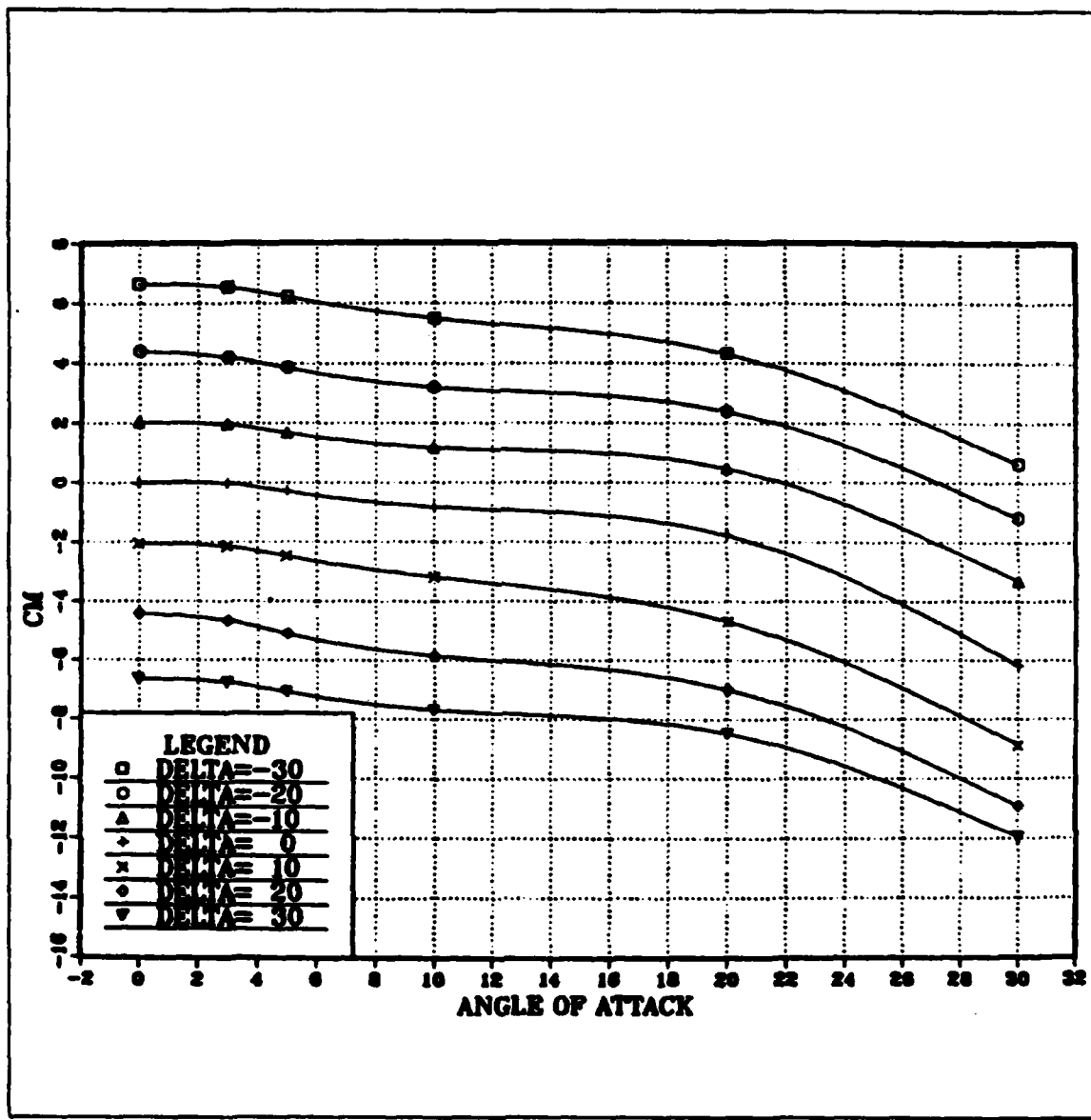
Figure 29.   Pitching Moment Coefficient versus Angle of Attack at Design Point
Three
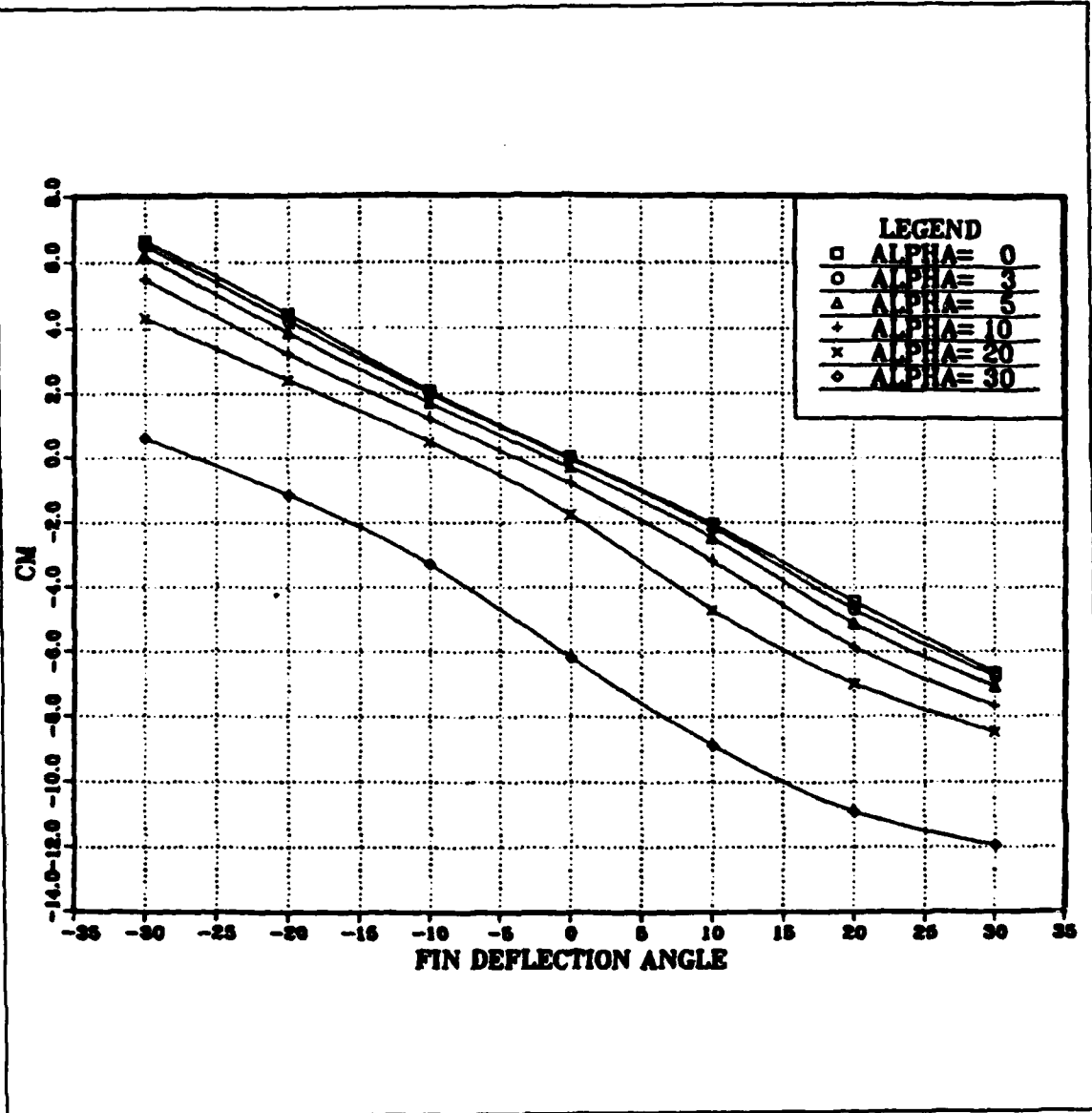
Figure 30.   Pitching Moment Coefficient versus Fin Deflection Angle at Design
Point Three

APPENDIX E. SIMULATION COMPUTER PROGRAM

```
**************************************************************
**************************************************************
***                                                    ***
***               THESIS RESEARCH                      ***
***                                                    ***
***          DSL SIMULATIONS FOR TWO                   ***
***          AUTOPILOT  CONFIGURATIONS                 ***
***           AT THREE DESIGN POINTS                   ***
***                                                    ***
***            KENNETH E.  COCKERHAM                   ***
***          CAPTAIN, UNITED STATES ARMY               ***
***                                                    ***
***          NAVAL POSTGRADUATE SCHOOL                 ***
***                                                    ***
**************************************************************
**************************************************************
*
*
*
FIXED INPUT
*RUN 1
******************DESIGN POINT ONE********************
*
******************MISSILE PARAMETERS******************
PARAM I = 720.0, M = 450.0, DAMP = -22.4, FLA = 799276.0, FLD = 88808.0
PARAM MPA = -168736.0, MPD = -191368.0
*
**********FEEDBACK GAINS FOR CONFIGURATION ONE**********
PARAM  KA1 = -0.094, KF1 = 27.6, KBR1 = 0.752, KST = 26.96
*
**********FEEDBACK GAINS FOR CONFIGURATION TWO**********
PARAM  KA2 = 1.0, KF2 = 20.1, KBR2 = -0.513
*
********FEED FORWARD GAINS FOR CONFIGURATION TWO********
PARAM  K1 = -0.094, K2 = 0.004
**************************************************************
*
*
*
*
*
*
DERIVATIVE
*
*
*************AUTOPILOT CONFIGURATION ONE*****************
*
*
        R1        = KA1 * STEP(0.0)
        X1        = R1 - X14 - X12
        X2        = INTGRL(0.0,X1)
        X3        = X2 - X11 - X13
```

```
        X4        = INTGRL(0.0,X3)
        X5        = X4
        DELTA1    = LIMIT(-0.35,0.35,X5)
        X6        = DELTA1 * MPD/I
        ALFDD1    = X6 + X7 + X8
        ALFD1     = INTGRL(0.0,ALFDD1)
        ALF1      = INTGRL(0.0,ALFD1)
        X7        = ALFD1 * DAMP
        X8        = ALF1 * (MPA+MPD)/I
        X9        = DELTA1 * FLD/M
        X10       = ALF1 * (FLA+FLD)/M
        ACCEL1    = X9 + X10
        X11       = KBR1 * ALFD1
        X12       = KST * X11
        X13       = KF1 * X4
        X14       = KA1 * ACCEL1
*
*
*
*
*****************AUTOPILOT CONFIGURATION TWO*****************
*
*
*
        R2        = KA2 * STEP(0.0)
        Y1        = R2 - Y16
        Y2        = K1 * Y1
        Y3        = INTGRL(0.0,Y2)
        Y4        = K2 * Y1
        Y5        = Y4 + Y3
        Y6        = Y5 - Y14 - Y15
        Y7        = INTGRL(0.0,Y6)
        Y8        = Y7
        DELTA2    = LIMIT(-0.35,0.35,Y8)
        Y9        = DELTA2 * MPD/I
        ALFDD2    = Y9 + Y10 + Y11
        ALFD2     = INTGRL(0.0,ALFDD2)
        ALF2      = INTGRL(0.0,ALFD2)
        Y10       = ALF2 * (MPA+MPD)/I
        Y11       = ALFD2 * DAMP
        Y12       = ALF2 * (FLA+FLD)/M
        Y13       = DELTA2 * FLD/M
        ACCEL2    = Y12 + Y13
        Y14       = ALFD2 * KBR2
        Y15       = Y7 * KF2
        Y16       = KA2 * ACCEL2
*
*
*
CONTROL FINTIM =2.0, DELT = 0.0001
*
*
SAVE 0.001, ACCEL1,ACCEL2
END
*
*
```

```
*
*
*RUN 2
*****************DESIGN POINT TWO*********************
****************MISSILE PARAMETERS*******************
PARAM I = 693, M = 370, DAMP = -11.9, FLA = 238350.0, FLD = 19080.0
PARAM MPA = -43545.0, MPD = -54431.0
*********FEEDBACK GAINS FOR CONFIGURATION ONE*********
PARAM  KA1 = -0.845, KF1 = 38.1, KBR1 = -4.44, KST = 8.98
*********FEEDBACK GAINS FOR CONFIGURATION TWO*********
PARAM  KA2 = 1.0, KF2 = 41.05, KBR2 = -7.62
*******FEED FORWARD GAINS FOR CONFIGURATION TWO*******
PARAM  K1 = -0.845, K2 = -0.057
*****************************************************
END
*
*
*
*
*RUN 3
***************DESIGN POINT THREE*********************
****************MISSILE PARAMETERS*******************
PARAM I = 687, M = 365, DAMP = -9.1, FLA = 99695.0, FLD = 10657.0
PARAM MPA = -26986.0, MPD = -29679.0
*********FEEDBACK GAINS FOR CONFIGURATION ONE*********
PARAM KA1 = -3.06, KF1 = 40.9, KBR1 = -12.37, KST = 10.18
*********FEEDBACK GAINS FOR CONFIGURATION TWO*********
PARAM  KA2 = 1.0, KF2 = 51.17, KBR2 = -12.83
*******FEED FORWARD GAINS FOR CONFIGURATION TWO*******
PARAM  K1 = -3.06, K2 = -0.352
*****************************************************
END
*
*
GRAPH (G1 ,DE=TEK618) TIME, ACCEL1(RU=1,LO=-0.2,SC=0.2)
LABEL (G1) STEP RESPONSE, CONFIGURATION 1, DESIGN POINT 1
*
GRAPH (G2 ,DE=TEK618) TIME, ACCEL1(RU=2)
LABEL (G2) STEP RESPONSE, CONFIGURATION 1, DESIGN POINT 2
*
GRAPH (G3 ,DE=TEK618) TIME, ACCEL1(RU=3)
LABEL (G3) STEP RESPONSE, CONFIGURATION 1, DESIGN POINT 3
*
GRAPH (G4 ,DE=TEK618) TIME, ACCEL1(RU=1,2,3)
LABEL (G4) STEP RESPONSE, CONFIGURATION 1, DESIGN POINTS 1, 2, & 3
*
GRAPH (G5 ,DE=TEK618) TIME, ACCEL2(RU=1)
LABEL (G5) STEP RESPONSE, CONFIGURATION 2, DESIGN POINT 1
*
GRAPH (G6 ,DE=TEK618) TIME, ACCEL2(RU=2)
LABEL (G6) STEP RESPONSE, CONFIGURATION 2, DESIGN POINT 2
*
GRAPH (G7 ,DE=TEK618) TIME, ACCEL2(RU=3)
LABEL (G7) STEP RESPONSE, CONFIGURATION 2, DESIGN POINT 3
*
GRAPH (G8 ,DE=TEK618) TIME, ACCEL2(RU=1,2,3)
```

```
LABEL (G8) STEP RESPONSE, CONFIGURATION 2,DESIGN POINTS 1, 2, & 3
*
GRAPH (G9 ,DE=TEK618) TIME, ACCEL1(RU=1,LO=-0.2,SC=0.2),ACCEL2(RU=1)
LABEL (G9) STEP RESPONSE, CONFIGURATIONS 1 & 2,DESIGN POINT 1
*
GRAPH (G10 ,DE=TEK618) TIME, ACCEL1(RU=2),ACCEL2(RU=2)
LABEL (G10) STEP RESPONSE, CONFIGURATIONS 1 & 2, DESIGN POINT 2
*
GRAPH (G11 ,DE=TEK618) TIME, ACCEL1(RU=3),ACCEL2(RU=3)
LABEL (G11) STEP RESPONSE, CONFIGURATIONS 1 & 2, DESIGN POINT 3
*
END
STOP
```

LIST OF REFERENCES

1. Dow, R.B., *Fundamentals of Advanced Missiles*, John Wiley & Sons, Inc., 1958.

2. Anderson, J.D., *Introduction to Flight*, pp. 387-393, McGraw-Hill Book Co., 1978.

3. *CRC Handbook of Chemistry and Physics*, 59th ed., p. F-209, CRC Press, Inc., 1979.

4. Nielsen, J.N., *Missile Aerodynamics*, pp. 259-260, McGraw-Hill Book Co., 1960.

5. Thaler, G.J., *Automatic Control Systems*, West Publishing Co., 1989.

6. Locke, A.S., *Guidance*, D. Van Nostrand Co., 1955.

7. Showalter, J.A., *Introduction to Defensive Missile Guidance & Control and Arming & Fuzing*, HRB-Singer, Inc., 1987.

8. International Business Machines, *Dynamic Simulation Language VS: Language Reference Manual*, IBM Corporation.

9. Reid, J.G., *Linear System Fundamentals; Continuous and Discrete, Classic and Modern*, McGraw-Hill Book Co., 1983.

INITIAL DISTRIBUTION LIST

		No. Copies
1.	Defense Technical Information Center Cameron Station Alexandria, VA 22304-6145	2
2.	Library, Code 0142 Naval Postgraduate School Monterey, CA 93943-5002	2
3.	Professor H. A. Titus, Code 62TS Department of Electrical and Computer Engineering Naval Postgraduate School Monterey, CA 93943	5
4.	Professor R. Cristi, Code 62CX Department of Electrical and Computer Engineering Naval Postgraduate School Monterey, CA 93943	1
5.	Chairman, Code 62 Department of Electrical and Computer Engineering Naval Postgraduate School Monterey, CA 93943	1
6.	Professor G.J. Thaler, Code 62TR Department of Electrical and Computer Engineering Naval Postgraduate School Monterey, CA 93943	1
7.	Dr. Jill Burt Missile and Space Intelligence Center Redstone Arsenal, AL 35898-5500	2
8.	Rear Admiral R. Gentz Commander Pacific Missile Test Center Point Mugu, CA 93042-5000	1
9.	Commander Naval Weapons Center ATTN: CODE 35405 China Lake, CA 93555-6001	1
10.	Commander Naval Air Test Center ATTN: SY94 Patuxent River, MD 20670-5304	1

11. Captain Kenneth Cockerham   2
    USA EHSC, Detachment II
    Fort Gillem, GA 30330

12. Lieutenant Ed Chaulk   1
    SMC #1285
    Naval Postgraduate School
    Monterey, CA 93943